Numer. Math. Theor. Meth. Appl.
doi: 10.4208/nmtma.2015.w11si

Vol. **8**, No. 2, pp. 253-282
May 2015

A FEM-Multigrid Scheme for Elliptic Nash-Equilibrium Multiobjective Optimal Control Problems

Mohammad Tanvir Rahman, Alfio Borzì*

Department of Mathematics, University of Würzburg, Emil-Fischer-Str. 30, 97074 Würzburg, Germany.

Received 15 August 2014; Accepted 18 September 2014

Abstract. A finite-element multigrid scheme for elliptic Nash-equilibrium multiobjective optimal control problems with control constraints is investigated. The multigrid computational framework implements a nonlinear multigrid strategy with collective smoothing for solving the multiobjective optimality system discretized with finite elements. Error estimates for the optimal solution and two-grid local Fourier analysis of the multigrid scheme are presented. Results of numerical experiments are presented to demonstrate the effectiveness of the proposed framework.

AMS subject classifications: 15A12; 65F10; 65F15
Key words: Elliptic partial differential equations, multigrid methods, Nash equilibrium, optimal control theory, finite element method.

1. Introduction

The simultaneous optimization of several objectives depending on different control mechanisms and subject to a unique model constraint defines a special class of multiobjective optimization problems. In the case of finite-dimensional models, a representative class of multiobjective optimization problems are game theory problems. In the infinite-dimensional case, multiobjective optimization usually refers to differential models. Specific infinite-dimensional application problems are aerodynamic shape optimization with the purpose of lift maximization and drag minimization [9, 11], and multi-loading structural design [17].

The pioneering results on finite-dimensional multiobjective optimization can be found in the works of Pareto, Nash, and Stackelberg; see e.g. [7, 8, 10]. On the other hand, the literature on infinite-dimensional multiobjective problems is much more recent and sparse. In particular, the Pareto solution concept may be found in, e.g., [12, 13], while much less is known regarding the Nash solution concept in multiobjective optimization problems governed by differential systems; see the very recent papers [1, 14, 15, 18]. Furthermore, it is only recently that efficient methods for

*Corresponding author. *Email address:* tanvir.rahman@mathematik.uni-wuerzburg.de (Mohammad Tanvir Rahman), alfio.borzi@mathematik.uni-wuerzburg.de (Alfio Borzì)

 ©2015 Global-Science Press

https://doi.org/10.4208/nmtma.2015.w11si Published online by Cambridge University Press

the solution of finite-dimensional Nash equilibrium problems have been investigated, whereas in the infinite-dimensional case the development and analysis of solution techniques is at its infancy. The purpose of this paper is to contribute to this development with a finite-element multigrid solution strategy for infinite-dimensional elliptic Nash-equilibrium multiobjective optimization problems. Specifically, we focus on an elliptic partial differential equation (PDE) with distributed controls and two objectives corresponding to two controls that are sought to obtain a Nash equilibrium. This setting is similar to that in [1, 14, 15], where finite-dimensional solution techniques are used to solve a finite-differences discretized multiobjective optimization problem. In contrast, we consider a FEM discretization and a multigrid solution strategy that is appropriate to solve elliptic PDE-optimization problems with optimal complexity at any mesh size. We remark that the present work addresses many novel issues. In fact, it considers a finite-element discretization of a Nash-equilibrium multiobjective optimality system in domains that are difficult to handle with finite differences and provides accuracy results for this setting. Further, it develops a powerful multigrid strategy that accommodates constraints on the control and is supported by local Fourier analysis results. However, while this paper provides a novel ground-making contribution to many different aspects of the numerical solution to elliptic Nash-equilibrium multiobjective optimization problems, many issue remain subject of further investigation. Therefore, we limit our theoretical analysis of the discretization to a one-dimensional setting and analyses the multigrid convergence only in the unconstrained case.

This paper is organized as follows. In Section 2, we formulate a class of elliptic Nash-equilibrium multiobjective optimization problems. We consider two objectives and two constrained controls that are defined in two subsets of the computational domain. Correspondingly, we introduce the optimality system that characterizes the solution to our multiobjective optimization problem. In Section 3, we illustrate a finite-element discretization of the optimality system and investigate the resulting approximation properties. We extend the analysis of [16] and prove $3/2$-order convergence for the control functions. In Section 4, we discuss a multigrid method for the solution of the optimality system. We present a full multigrid scheme with collective smoothing that is able to accommodate the presence of inequality constraints. The optimal convergence properties of our multigrid scheme are investigated in Section 5 using local Fourier analysis. In Section 6, we present results of numerical experiments to validate our Nash-equilibrium optimal control framework. In particular, we validate the theoretical estimates and the computational performance of the proposed FEM-multigrid scheme. Our FEM multigrid scheme is found to be efficient and robust for a large range of the weights of the costs of the controls and provides second-order optimal solutions. A section of conclusions completes this work.

2. An elliptic multiobjective optimal control problem

In this section, we formulate a class of elliptic multiobjective Nash-equilibrium distributed control problems as follows.

https://doi.org/10.4208/nmtma.2015.w11si Published online by Cambridge University Press

Find $(u_1, u_2) \in \mathcal{U}_{ad,1} \times \mathcal{U}_{ad,1} \subset L^2(\Omega) \times L^2(\Omega)$ such that

$$\begin{array}{ll} \min\limits_{y,u_1} J_1(y, u_1, u_2) & \\ \min\limits_{y,u_2} J_2(y, u_1, u_2) & \\ -\Delta y \;=\; B_1 u_1 + B_2 u_2 & \text{in } \Omega, \\ y \;=\; 0 & \text{on } \partial\Omega, \\ u_1 \;\in\; \mathcal{U}_{ad,1},\; u_2 \;\in\; \mathcal{U}_{ad,2}, & \end{array} \tag{2.1}$$

where the objectives are given by

$$J_j(y, u_1, u_2) := \frac{1}{2} \parallel y - z_j \parallel^2_{L^2(\Omega)} + \frac{\nu_j}{2} \parallel B_j u_j \parallel^2_{L^2(\Omega)}, \quad j = 1, 2. \tag{2.2}$$

The functions $z_1, z_2 \in L^2(\Omega)$ are given target functions and the parameters $\nu_j > 0$, $j = 1, 2$, represent the weights of the costs of the controls.

The set of admissible controls $\mathcal{U}_{ad} = \mathcal{U}_{ad,1} \times \mathcal{U}_{ad,2}$ is the space product of two closed convex subsets of $L^2(\Omega)$ given by

$$\mathcal{U}_{ad,j} = \Big\{ u \in L^2(\omega_j) \mid a_j \;\leq u(x) \;\leq b_j \quad \text{a.e. in } \omega_j \subset \Omega \Big\}, \tag{2.3}$$

where the $a_j < b_j$, for $j = 1, 2$, are elements of $L^\infty(\omega_j)$ and the ω_j are open, possibly disjoint subsets of Ω, where the controls are defined. The linear operators $B_j : L^2(\omega_j) \to L^2(\Omega)$ are extension operators (by zero) given by

$$B_j u_j \;= \begin{cases} u_j & \text{in } \omega_j \\ 0 & \text{in } \Omega \setminus \omega_j. \end{cases} \tag{2.4}$$

We assume that for given $(u_1, u_2) \in \mathcal{U}_{ad}$, the solution to the state equation

$$\begin{array}{ll} -\Delta y = B_1 u_1 + B_2 u_2 & \text{in } \Omega, \\ y = 0 & \text{on } \partial\Omega, \end{array} \tag{2.5}$$

admits a unique solution $y = y(u_1, u_2) \in H^1_0(\Omega) \cap H^2(\Omega)$. With our setting, the mapping $(u_1, u_2) \longmapsto y$ is affine and differentiable. In order to define a suitable solution concept for the elliptic multiobjective optimization problem (2.1), we define the following reduced cost functionals

$$\hat{J}_j(u_1, u_2) \;=\; J_j(y(u_1, u_2), u_1, u_2), \quad j = 1, 2.$$

In terms of the reduced objectives, we can reformulate problem (2.1) as follows

$$(\hat{P}) \qquad \begin{cases} \min\limits_{u_1} \hat{J}_1(u_1, u_2) & \text{s.t.} \quad u_1 \;\in\; \mathcal{U}_{ad,1} \\ \min\limits_{u_2} \hat{J}_2(u_1, u_2) & \text{s.t.} \quad u_2 \;\in\; \mathcal{U}_{ad,2} \end{cases} \tag{2.6}$$

With this formulation, we can introduce the following Nash solution concept similar to [1]. We have

https://doi.org/10.4208/nmtma.2015.w11si Published online by Cambridge University Press

Definition 2.1. *A feasible element $\bar{u} = (\bar{u}_1, \bar{u}_2) \in \mathcal{U}_{ad}$ is called a Nash solution or a Nash equilibrium of $(\hat{P})$, if*

$$\begin{aligned} \hat{J}_1(\bar{u}_1, \bar{u}_2) &\leq \hat{J}_1(u_1, \bar{u}_2) \quad \textit{for all} \quad u_1 \in \mathcal{U}_{ad,1}, \\ \hat{J}_2(\bar{u}_1, \bar{u}_2) &\leq \hat{J}_2(\bar{u}_1, u_2) \quad \textit{for all} \quad u_2 \in \mathcal{U}_{ad,2}. \end{aligned}$$

The triple $(\bar{y}, \bar{u}_1, \bar{u}_2)$ represents a Nash-equilibrium of the multiobjective optimization problem (2.1) if $(\bar{u}_1, \bar{u}_2)$ is a Nash equilibrium for the reduced problem $(\hat{P})$ and $\bar{y} = y(\bar{u}_1, \bar{u}_2)$.

The first-order optimality condition for the Nash-equilibrium multiobjective control problem that characterizes the optimal solution $(\bar{u}_1, \bar{u}_2) \in \mathcal{U}_{ad}$ is given by

$$\frac{\partial \hat{J}_1}{\partial u_1}(\bar{u}_1, \bar{u}_2)(v_1 - \bar{u}_1) \geq 0 \quad \forall v_1 \in \mathcal{U}_{ad,1}, \tag{2.7}$$

$$\frac{\partial \hat{J}_2}{\partial u_2}(\bar{u}_1, \bar{u}_2)(v_2 - \bar{u}_2) \geq 0 \quad \forall v_2 \in \mathcal{U}_{ad,2}. \tag{2.8}$$

Now, let us introduce the operator S, representing the inverse of the minus Laplacian with homogeneous Dirichlet boundary conditions. We have that the solution to (2.5) corresponds to the following

$$y = S(B_1 u_1 + B_2 u_2). \tag{2.9}$$

Henceforth, we compute the derivatives of the reduced functionals with respect to the control variables. We have

$$\begin{aligned} &\frac{\partial \hat{J}_1}{\partial u_1}(\bar{u}_1, \bar{u}_2)(\delta \bar{u}_1) = (\nabla_{u_1} \hat{J}_1(\bar{u}_1, \bar{u}_2), \delta \bar{u}_1) \\ &= \lim_{\alpha \to 0^+} \frac{1}{\alpha} (\hat{J}_1(\bar{u}_1 + \alpha \delta \bar{u}_1, \bar{u}_2) - \hat{J}_1(\bar{u}_1, \bar{u}_2)) \\ &= \lim_{\alpha \to 0^+} \frac{1}{\alpha} \{ \frac{1}{2} \parallel S(B_1(\bar{u}_1 + \alpha \delta \bar{u}_1) + B_2 \bar{u}_2) - z_1 \parallel^2_{L^2(\Omega)} + \frac{\nu_1}{2} \parallel B_1(\bar{u}_1 + \alpha \delta \bar{u}_1) \parallel^2_{L^2(\Omega)} \\ &\qquad - \frac{1}{2} \parallel S(B_1 \bar{u}_1 + B_2 \bar{u}_2) - z_1 \parallel^2_{L^2(\Omega)} - \frac{\nu_1}{2} \parallel B_1 \bar{u}_1 \parallel^2_{L^2(\Omega)} \} \\ &= (S B_1 \bar{u}_1 + S B_2 \bar{u}_2 - z_1 \ , \ S B_1 \delta \bar{u}_1)_{L^2(\Omega)} + (\nu_1 B_1 \bar{u}_1 \ , \ B_1 \delta \bar{u}_1)_{L^2(\Omega)} \\ &= (B_1^* S^* (S B_1 \bar{u}_1 + S B_2 \bar{u}_2 - z_1) \ , \ \delta \bar{u}_1)_{L^2(\omega_1)} + (\nu_1 B_1^* B_1 \bar{u}_1 \ , \ \delta \bar{u}_1)_{L^2(\omega_1)}, \end{aligned}$$

where B_1^* and S^* are the adjoint operators corresponding to B_1 and S, respectively; notice that $S^* = S$. Similarly, we determine $\dfrac{\partial \hat{J}_2}{\partial u_2}$. Therefore because of (2.7)-(2.8), we obtain the first-order optimality conditions as follows

$$\begin{aligned} &(B_1^* S^* (S B_1 \bar{u}_1 + S B_2 \bar{u}_2 - z_1) + \nu_1 B_1^* B_1 \bar{u}_1, v_1 - \bar{u}_1)_{L^2(\omega_1)} \geq 0 \quad \forall v_1 \in \mathcal{U}_{ad,1}, \\ &(B_2^* S^* (S B_1 \bar{u}_1 + S B_2 \bar{u}_2 - z_2) + \nu_1 B_2^* B_2 \bar{u}_2, v_2 - \bar{u}_2)_{L^2(\omega_2)} \geq 0 \quad \forall v_2 \in \mathcal{U}_{ad,2}. \end{aligned} \tag{2.10}$$

https://doi.org/10.4208/nmtma.2015.w11si Published online by Cambridge University Press

Next, we introduce the adjoint variables $p_1, p_2 \in H^2(\Omega) \cap H_0^1(\Omega)$ defined as follows

$$\begin{array}{ll} p_j = S^*(SB_1u_1 + SB_2u_2 - z_j) & \text{in } \Omega \\ p_j = 0 & \text{on } \partial\Omega \end{array} \tag{2.11}$$

where $j = 1, 2$. Using these Lagrange multipliers, we obtain the first-order optimality conditions in the following from

$$\begin{array}{ll} (B_1^* \bar{p}_1 + \nu_1 B_1^* B_1 \bar{u}_1, v_1 - \bar{u}_1)_{L^2(\omega_1)} \geq 0 & \forall v_1 \in \mathcal{U}_{ad,1}, \\ (B_2^* \bar{p}_2 + \nu_1 B_2^* B_2 \bar{u}_2, v_2 - \bar{u}_2)_{L^2(\omega_2)} \geq 0 & \forall v_2 \in \mathcal{U}_{ad,2}, \end{array} \tag{2.12}$$

where $\bar{p}_j = p_j(\bar{u}_1, \bar{u}_2)$, $j = 1, 2$.

Summarizing, we have the following optimality system that characterizes the Nash-equilibrium solution to the optimal control problem (2.1).

$$\begin{array}{ll} -\Delta y = B_1u_1 + B_2u_2 & \text{in } \Omega, \\ y = 0 & \text{on } \partial\Omega, \\ -\Delta p_1 = (y - z_1) & \text{in } \Omega, \\ p_1 = 0 & \text{on } \partial\Omega, \\ -\Delta p_2 = (y - z_2) & \text{in } \Omega, \\ p_2 = 0 & \text{on } \partial\Omega, \\ (B_1^* p_1 + \nu_1 B_1^* B_1 u_1, v_1 - u_1) \geq 0 & \forall v_1 \in \mathcal{U}_{ad,1}, \\ (B_2^* p_2 + \nu_1 B_2^* B_2 u_2, v_2 - u_2) \geq 0 & \forall v_2 \in \mathcal{U}_{ad,2}. \end{array} \tag{2.13}$$

3. A FEM discretization

In this section, we discuss a linear finite-element (FEM) discretization of the optimality system (2.13). For simplicity, we assume a one-dimensional space problem in $\Omega = (a, b)$. However, our discussion is valid also in a two-dimensional convex smooth domain. We subdivide the interval (a, b) in n sub-intervals with mesh size $h = (b-a)/n$, and grid points $x_i = ih$, $i = 0, \ldots, n$.

In a FEM context, we use the standard linear basis functions e_i, $i = 1, \ldots, n-1$, and the following weak formulation of the state equation

$$\int_\Omega \nabla y \cdot \nabla w \, dx = \int_\Omega (B_1u_1 + B_2u_2)\, w \, dx. \tag{3.1}$$

Next, we introduce a finite-dimensional subspace for y, u_1 and u_2 with dimension $n-1$ which is spanned by the linearly independent basis functions e_i. We obtain the following discrete approximation to the state and control functions

$$y^h(x) = \sum_{k=1}^{n-1} Y_k e_k(x), \qquad u_j^h(x) = \sum_{k=1}^{n-1} U_{j,k} e_k(x) \quad \text{for } j = 1, 2.$$

https://doi.org/10.4208/nmtma.2015.w11si Published online by Cambridge University Press

and

$$B_j^h U_{j,k} = \begin{cases} U_{j,k} & \text{if } x_k \in \omega_j \\ 0 & \text{otherwise.} \end{cases} \tag{3.2}$$

We have that $Y = (Y_1, \ldots, Y_{n-1})$, and $U_j = (U_{j,1}, \ldots, U_{j,n-1})$ for $k = 1, ..., n-1$ and $j = 1, 2$, represent the unknowns of the problem. With this setting, our state Eq. (3.1) results in the following

$$KY = M(B_1^h U_1 + B_2^h U_2), \tag{3.3}$$

where K and M denote the stiffness matrix and the mass matrix, respectively.

Further, we obtain the following discrete adjoint equations

$$KP_1 = MY - Z_1 \tag{3.4}$$
$$KP_2 = MY - Z_2 \tag{3.5}$$

where $Z_j = (Z_{j,1}, \ldots, Z_{j,n-1})$ with

$$Z_{j,i} = \int_\Omega z_j e_i \, dx \quad j = 1, 2, \quad i = 1, \ldots, n-1.$$

Summarizing, we have the following discrete optimality system

$$\begin{aligned} &KY = M(B_1^h U_1 + B_2^h U_2), \\ &KP_1 = MY - Z_1, \\ &KP_2 = MY - Z_2, \\ &(B_1^{*h}(P_1 + \nu_1 U_1), \Phi_1 - U_1) \geq 0 \quad \forall \Phi_1 \in \mathcal{U}_{k,1}, \\ &(B_2^{*h}(P_2 + \nu_2 U_2), \Phi_2 - U_2) \geq 0 \quad \forall \Phi_2 \in \mathcal{U}_{k,2}. \end{aligned} \tag{3.6}$$

Here B_j^{*h} is the discrete version of the operator of B_j^*, which is $B_j^{*h} = (B_j^h)^T$.

In the remaining of this section, we investigate the accuracy of the FEM solution to this multiobjective optimality system. For this purpose, we extend the approach in [16] to our case with two localized controls and two objectives.

We start assuming that we can solve the state equation and the adjoint equations with a certain accuracy $\tilde{\delta}_1$ and $\tilde{\delta}_2$ corresponding to $\tilde{f}_1$ and $\tilde{f}_2$, that represent the deviation of the numerical solutions to the solutions of the original problem. As a preparation for our analysis, we prove the following Lemma.

Lemma 3.1. *Let $(\tilde{u}_1^h, \tilde{u}_2^h)$ satisfy the following inequality constraints*

$$(B_j^* S^*(S(\, B_1 \tilde{u}_1^h + B_2 \tilde{u}_2^h\,) - z_j) + B_j^* \tilde{f}_j + \nu_j B_j^* B_j \tilde{u}_j^h, v_j^h - \tilde{u}_j^h)_{L^2(\omega_j)} \geq 0$$

for all $v_j^h \in \mathcal{U}_{ad,jh}$, $j = 1, 2$, and assume

$$\| \, \tilde{f}_j \, \|_{L^2(\Omega)} \leq \tilde{\delta}_j, \qquad j = 1, 2.$$

https://doi.org/10.4208/nmtma.2015.w11si Published online by Cambridge University Press

Then the error estimate

$$\| \bar{u}_1 - \tilde{u}_1^h \|_{L^2(\omega_1)} + \| \bar{u}_2 - \tilde{u}_2^h \|_{L^2(\omega_2)} \leq C(\tilde{\delta}_1 + \tilde{\delta}_2)$$

holds true.

Proof. We test the variational inequality for $\tilde{u}_j^h$ with $\bar{u}_j$ and the original inequality constraints (2.10) with $\tilde{u}_j^h$. We have

$$\begin{aligned}
&(B_j^* S^*(S(\, B_1\tilde{u}_1^h + B_2\tilde{u}_2^h\,) - z_j) + B_j^*\tilde{f}_j + \nu_j B_j^* B_j\tilde{u}_j^h, \bar{u}_j - \tilde{u}_j^h)_{L^2(\omega_j)} \geq 0,\\
&(B_j^* S^*(S(\, B_1\bar{u}_1 + B_2\bar{u}_2\,) - z_j) + \nu_j B_j^* B_j\bar{u}_j, \tilde{u}_j^h - \bar{u}_j)_{L^2(\omega_j)} \geq 0,
\end{aligned}$$

for $j = 1, 2$. We add these two inequalities and obtain

$$(B_j^* S^*(S(\, B_1(\tilde{u}_1^h - \bar{u}_1) + B_2(\tilde{u}_2^h - \bar{u}_2)\,) + B_j^*\tilde{f}_j + \nu_j B_j^* B_j(\tilde{u}_j^h - \bar{u}_j), \bar{u}_j - \tilde{u}_j^h)_{L^2(\omega_j)} \geq 0$$

where $j = 1, 2$. After some rearrangements, we obtain

$$\begin{aligned}
&(\nu_1 B_1^* B_1(\bar{u}_1 - \tilde{u}_1^h), \bar{u}_1^h - \tilde{u}_1^h)_{L^2(\omega_1)} + (B_1^* S^*(S(\, B_1(\bar{u}_1 - \tilde{u}_1^h) + B_2(\bar{u}_2 - \tilde{u}_2^h)\,), \bar{u}_1 - \tilde{u}_1^h)_{L^2(\omega_1)}\\
&\leq (B_1^*\tilde{f}_1, \bar{u}_1 - \tilde{u}_1^h)_{L^2(\omega_1)}\\
&(\nu_2 B_2^* B_2(\bar{u}_2 - \tilde{u}_2^h), \bar{u}_2 - \tilde{u}_2^h)_{L^2(\omega_2)} + (B_2^* S^*(S(\, B_1(\bar{u}_1 - \tilde{u}_1^h) + B_2(\bar{u}_2 - \tilde{u}_2^h)\,), \bar{u}_2 - \tilde{u}_2^h)_{L^2(\omega_2)}\\
&\leq (B_2^*\tilde{f}_2, \bar{u}_2 - \tilde{u}_2^h)_{L^2(\omega_2)}
\end{aligned}$$

We add these two inequalities together and obtain

$$\begin{aligned}
&(\nu_1 B_1(\bar{u}_1 - \tilde{u}_1^h), B_1(\bar{u}_1 - \tilde{u}_1^h))_{L^2(\Omega)} + (\nu_2 B_2(\bar{u}_2 - \tilde{u}_2^h), B_2(\bar{u}_2 - \tilde{u}_2^h))_{L^2(\Omega)}\\
&\quad + (S(B_1(\bar{u}_1 - \tilde{u}_1^h), S(B_1(\bar{u}_1 - \tilde{u}_1^h))_{L^2(\Omega)} + (S(B_2(\bar{u}_2 - \tilde{u}_2^h), S(B_2(\bar{u}_2 - \tilde{u}_2^h))_{L^2(\Omega)}\\
&\quad + 2\,(S(\, B_1(\bar{u}_1 - \tilde{u}_1^h), S(\, B_2(\bar{u}_2 - \tilde{u}_2^h))_{L^2(\Omega)}\\
&\leq (\tilde{f}_1, B_1(\bar{u}_1 - \tilde{u}_1^h))_{L^2(\Omega)} + (\tilde{f}_2, B_2(\bar{u}_2 - \tilde{u}_2^h))_{L^2(\Omega)}.
\end{aligned}$$

We have the following

$$\begin{aligned}
&\nu_1 \| B_1(\bar{u}_1 - \tilde{u}_1^h) \|^2_{L^2(\Omega)} + \nu_2 \| B_2(\bar{u}_2 - \tilde{u}_2^h) \|^2_{L^2(\Omega)} + \| S(\, B_1(\bar{u}_1 - \tilde{u}_1^h) + B_2(\bar{u}_2 - \tilde{u}_2^h)\,) \|^2_{L^2(\Omega)}\\
&\leq \| \tilde{f}_1 \|_{L^2(\Omega)} \| B_1(\bar{u}_1 - \tilde{u}_1^h) \|_{L^2(\Omega)} + \| \tilde{f}_2 \|_{L^2(\Omega)} \| B_2(\bar{u}_2 - \tilde{u}_2^h) \|_{L^2(\Omega)}\,.
\end{aligned}$$

Now, we take $\epsilon < \min(\nu_1, \nu_2)$ and use the Cauchy inequality.

$$\begin{aligned}
&\nu_1 \| B_1(\bar{u}_1 - \tilde{u}_1^h) \|^2_{L^2(\Omega)} + \nu_2 \| B_2(\bar{u}_2 - \tilde{u}_2^h) \|^2_{L^2(\Omega)}\\
\leq &\frac{1}{4\epsilon} \| \tilde{f}_1 \|^2_{L^2(\Omega)} + \epsilon \| B_1(\bar{u}_1 - \tilde{u}_1^h) \|^2_{L^2(\Omega)}\\
&+ \frac{1}{4\epsilon} \| \tilde{f}_2 \|^2_{L^2(\Omega)} + \epsilon \| B_2(\bar{u}_2 - \tilde{u}_2^h) \|^2_{L^2(\Omega)}\,.
\end{aligned}$$

https://doi.org/10.4208/nmtma.2015.w11si Published online by Cambridge University Press

Therefore, we have the following

$$\begin{aligned}&(\nu_1-\epsilon)\parallel B_1(\bar{u}_1-\tilde{u}_1^h)\parallel^2_{L^2(\Omega)}+(\nu_2-\epsilon)\parallel B_2(\bar{u}_2-\tilde{u}_2^h)\parallel^2_{L^2(\Omega)}\\ \leq&\frac{1}{4\epsilon}\parallel\tilde{f}_1\parallel^2_{L^2(\Omega)}+\frac{1}{4\epsilon}\parallel\tilde{f}_2\parallel^2_{L^2(\Omega)}.\end{aligned}$$

Next, we use the following estimates

$$\begin{aligned}&\frac{1}{2}(\sqrt{\nu_1-\epsilon}\parallel B_1(\bar{u}_1-\tilde{u}_1^h)\parallel_{L^2(\Omega)}+\sqrt{\nu_2-\epsilon}\parallel B_2(\bar{u}_2-\tilde{u}_2^h)\parallel_{L^2(\Omega)})^2\\ \leq&(\nu_1-\epsilon)\parallel B_1(\bar{u}_1-\tilde{u}_1^h)\parallel^2_{L^2(\Omega)}+(\nu_2-\epsilon)\parallel B_2(\bar{u}_2-\tilde{u}_2^h)\parallel^2_{L^2(\Omega)}\end{aligned}$$

and

$$\frac{1}{4\epsilon}\left(\parallel\tilde{f}_1\parallel^2_{L^2(\Omega)}+\parallel\tilde{f}_2\parallel^2_{L^2(\Omega)}\right)\leq\frac{1}{4\epsilon}\left(\parallel\tilde{f}_1\parallel_{L^2(\Omega)}+\parallel\tilde{f}_2\parallel_{L^2(\Omega)}\right)^2.$$

We obtain

$$\begin{aligned}&\sqrt{\nu_1-\epsilon}\parallel B_1(\bar{u}_1-\tilde{u}_1^h)\parallel_{L^2(\Omega)}+\sqrt{\nu_2-\epsilon}\parallel B_2(\bar{u}_2-\tilde{u}_2^h)\parallel_{L^2(\Omega)}\\ \leq&\frac{1}{\sqrt{2\epsilon}}\left(\parallel\tilde{f}_1\parallel_{L^2(\Omega)}+\parallel\tilde{f}_2\parallel_{L^2(\Omega)}\right).\end{aligned}$$

Further, we define $C=\frac{1}{\min(\sqrt{\nu_1-\epsilon},\sqrt{\nu_2-\epsilon})}\frac{1}{\sqrt{2\epsilon}}$ and obtain the following estimate

$$\parallel\bar{u}_1-\tilde{u}_1^h\parallel_{L^2(\omega_1^h)}+\parallel\bar{u}_2-\tilde{u}_2^h\parallel_{L^2(\omega_2^h)}\leq C(\parallel\tilde{f}_1\parallel_{L^2(\Omega)}+\parallel\tilde{f}_2\parallel_{L^2(\Omega)})$$

that implies the assertion. □

To proceed further, we need the following two assumptions. We assume that there exists a finite number of points P, supposedly less than the discretization points but coinciding on them, such that $t^k\in[a,b]\,(k=0,\ldots,P,$ with $t^0=a,t^P=b)$.

Assumption 3.1. *The optimal controls $\bar{u}_1,\bar{u}_2$ of* (2.1) *are Lipschitz continuous and piecewise of class C^2, such that $\bar{u}_1\in C^2[t^{k-1},t^k]$ for all $k=1,\ldots,P_{u_1}$ and $\bar{u}_2\in C^2[t^{k-1},t^k]$ for all $k=1,\ldots,P_{u_2}$.*

For the adjoint variables, $(\bar{p}_1,\bar{p}_2)$ defined as follows

$$\bar{p}_j=S^*(SB_1\bar{u}_1+SB_2\bar{u}_2-z_j)\qquad\text{for } j=1,2\,,$$

we also need the following assumption.

Assumption 3.2. *The adjoint states $(\bar{p}_1,\bar{p}_2)$ of* (2.1) *are Lipschitz continuous and piecewise of class C^2, such that $\bar{p}_1\in C^2[t^{k-1},t^k]$ for all $k=1,\ldots,P_{p_1}$ and $\bar{p}_2\in C^2[t^{k-1},t^k]$ for all $k=1,\ldots,P_{p_2}$.*

https://doi.org/10.4208/nmtma.2015.w11si Published online by Cambridge University Press

Next, we consider (v_1, v_2), as the linear interpolate of the optimal solution $(\bar{u}_1, \bar{u}_2)$ of (2.1). We have

$$v_j = \sum_{i=1}^{n-1} \bar{u}_j(t_i)e_i \qquad \text{for } j = 1, 2.$$

Using Assumption 3.1, we can prove the following estimate

$$\| \bar{u}_1 - v_1 \|_{L^2(\omega_1)} = \| B_1(\bar{u}_1 - v_1) \|_{L^2(\Omega)} \leq c_1 \cdot h^{3/2} \tag{3.7a}$$

$$\| \bar{u}_2 - v_2 \|_{L^2(\omega_2)} = \| B_2(\bar{u}_2 - v_2) \|_{L^2(\Omega)} \leq c_2 \cdot h^{3/2}. \tag{3.7b}$$

The constants c_1, c_2 can be estimated by

$$c_1 \leq \frac{T}{8}C_1 + \frac{L_1}{2}\sqrt{M_1 - 1}, \quad c_2 \leq \frac{T}{8}C_2 + \frac{L_2}{2}\sqrt{M_2 - 1},$$

with

$$C_1 = \max_{k=1..M_1} \| \bar{u}_1'' \|_{C[t^{k-1}, t^k]}, \quad C_2 = \max_{k=1..M_2} \| \bar{u}_2'' \|_{C[t^{k-1}, t^k]},$$

where L_1, L_2 are the Lipschitz constants of $\bar{u}_1$ and $\bar{u}_2$ in ω_1 and ω_2 respectively. $T = b - a$ is the length of the domain and M_1 and M_2 are the number of points in ω_1 and ω_2 such that $\bar{u}_1$ and $\bar{u}_2$ are of class of C^2 in between. The details of the proof of the estimate above can be found in [16].

Lemma 3.2. *Let $(\bar{u}_1, \bar{u}_2)$ is the optimal solution of* (2.1) *satisfying Assumption* 3.1 *and (v_1, v_2) is its linear interpolate. If (u_1^h, u_2^h) is the solution to (P_h), then the following estimate holds true.*

$$\begin{aligned}
&(S^*(S(B_1\bar{u}_1 + B_2\bar{u}_2) - z_1) + \nu_1 B_1 u_1^h, B_1(v_1 - u_1^h))_{L^2(\Omega)} \\
&\quad + (S^*(S(B_2\bar{u}_1 + B_2\bar{u}_2) - z_2) + \nu_2 B_2 u_2^h, B_2(v_2 - u_2^h))_{L^2(\Omega)} \\
&\quad + c_4 h^{3/2} (\| B_1(v_1 - u_1^h) \|_{L^2(\Omega)} + \| B_2(v_2 - u_2^h) \|_{L^2(\Omega)}) \geq 0,
\end{aligned} \tag{3.8}$$

where $c_4 = c_3 \| S^*S \|_{\mathcal{L}(\Omega)}$.

Proof. As (v_1, v_2) is the linear interpolate of the optimal solution $\bar{u}_1, \bar{u}_2$, we obtain the following

$$\| B_1(\bar{u}_1 - v_1) \|_{L^2(\Omega)} + \| B_2(\bar{u}_2 - v_2) \|_{L^2(\Omega)} \leq c_3 h^{3/2},$$

where $c_3 = c_1 + c_2$. Therefore we have

$$\| B_1(\bar{u}_1 - v_1) + B_2(\bar{u}_2 - v_2) \|_{L^2(\Omega)} \leq c_3 h^{3/2}.$$

https://doi.org/10.4208/nmtma.2015.w11si Published online by Cambridge University Press

Further, we have

$$\begin{aligned}
&(S^*(S(B_1\bar{u}_1 + B_2\bar{u}_2) - z_1) + \nu_1 B_1\bar{u}_1^h, B_1(v_1 - u_1^h))_{L^2(\Omega)} \\
&\quad + (S^*(S(B_2\bar{u}_1 + B_2\bar{u}_2) - z_2) + \nu_2 B_2\bar{u}_2^h, B_2(v_2 - u_2^h))_{L^2(\Omega)} \\
&= (S^*(S(B_1(\bar{u}_1 - u_1^h) + B_2(\bar{u}_2 - u_2^h)) - z_1) + S(B_1u_1^h + B_2u_2^h) \\
&\quad + \nu_1 B_1\bar{u}_1^h, B_1(v_1 - u_1^h))_{L^2(\Omega)} + (S^*(S(B_1(\bar{u}_1 - u_1^h) + B_2(\bar{u}_2 - u_2^h)) - z_2) \\
&\quad + S(B_1u_1^h + B_2u_2^h) + \nu_2 B_2\bar{u}_2^h, B_2(v_2 - u_2^h))_{L^2(\Omega)} \\
&= (S^*S(B_1(\bar{u}_1 - u_1^h) + B_2(\bar{u}_2 - u_2^h)), B_1(v_1 - u_1^h))_{L^2(\Omega)} \\
&\quad + (S^*S(B_1(\bar{u}_1 - u_1^h) + B_2(\bar{u}_2 - u_2^h)), B_2(v_2 - u_2^h))_{L^2(\Omega)} \\
&\quad + (S^*(S(B_1u_1^h + B_2u_2^h) - z_1) + \nu_1 B_1\bar{u}_1^h, B_1(v_1 - u_1^h))_{L^2(\Omega)} \\
&\quad + (S^*(S(B_1u_1^h + B_2u_2^h) - z_2) + \nu_2 B_2\bar{u}_2^h, B_2(v_2 - u_2^h))_{L^2(\Omega)}
\end{aligned}$$

As we have

$$\begin{aligned}
&(S^*(S(B_1u_1^h + B_2u_2^h) - z_1) + \nu_1 B_1\bar{u}_1^h, B_1(v_1 - u_1^h))_{L^2(\Omega)} \geq 0, \\
&(S^*(S(B_1u_1^h + B_2u_2^h) - z_2) + \nu_2 B_2\bar{u}_2^h, B_2(v_2 - u_2^h))_{L^2(\Omega)} \geq 0,
\end{aligned}$$

we obtain the following inequality

$$\begin{aligned}
&(S^*(S(B_1\bar{u}_1 + B_2\bar{u}_2) - z_1) + \nu_1 B_1\bar{u}_1^h, B_1(v_1 - u_1^h))_{L^2(\Omega)} \\
&+ (S^*(S(B_2\bar{u}_1 + B_2\bar{u}_2) - z_2) + \nu_2 B_2\bar{u}_2^h, B_2(v_2 - u_2^h))_{L^2(\Omega)} \\
&\geq (S^*S(B_1(\bar{u}_1 - u_1^h) + B_2(\bar{u}_2 - u_2^h)), B_1(v_1 - u_1^h) + B_2(v_2 - u_2^h))_{L^2(\Omega)}
\end{aligned}$$

We proceed further as follows

$$\begin{aligned}
&(S^*S(B_1(\bar{u}_1 - u_1^h) + B_2(\bar{u}_2 - u_2^h)), B_1(v_1 - u_1^h) + B_2(v_2 - u_2^h))_{L^2(\Omega)} \\
&= (S^*S(B_1(\bar{u}_1 - v_1 + v_1 - u_1^h) + B_2(\bar{u}_2 - v_2 + v_2 - u_2^h)), \\
&\qquad B_1(v_1 - u_1^h) + B_2(v_2 - u_2^h))_{L^2(\Omega)} \\
&= (S^*S(B_1(\bar{u}_1 - v_1) + B_2(\bar{u}_2 - v_2)), B_1(v_1 - u_1^h) + B_2(v_2 - u_2^h))_{L^2(\Omega)} \\
&\quad + (S^*S(B_1(v_1 - u_1^h) + B_2(v_2 - u_2^h)), B_1(v_1 - u_1^h) + B_2(v_2 - u_2^h))_{L^2(\Omega)} \\
&= (S^*S(B_1(\bar{u}_1 - v_1) + B_2(\bar{u}_2 - v_2)), B_1(v_1 - u_1^h) + B_2(v_2 - u_2^h))_{L^2(\Omega)} \\
&\quad + \| S(B_1(v_1 - u_1^h) + B_2(v_2 - u_2^h)) \|^2_{L^2(\Omega)} \\
&\geq (S^*S(B_1(\bar{u}_1 - v_1) + B_2(\bar{u}_2 - v_2)), B_1(v_1 - u_1^h) + B_2(v_2 - u_2^h))_{L^2(\Omega)} \\
&\geq - \| S^*S \|_{\mathcal{L}(\Omega)} \| B_1(\bar{u}_1 - v_1) + B_2(\bar{u}_2 - v_2) \|_{L^2(\Omega)} \\
&\qquad \cdot \| B_1(v_1 - u_1^h) + B_2(v_2 - u_2^h) \|_{L^2(\Omega)} \\
&\geq - \| S^*S \|_{\mathcal{L}(\Omega)} c_3 h^{3/2} \| B_1(v_1 - u_1^h) + B_2(v_2 - u_2^h) \|_{L^2(\Omega)} \\
&\geq - \| S^*S \|_{\mathcal{L}(\Omega)} c_3 h^{3/2} (\| B_1(v_1 - u_1^h) \|_{L^2(\Omega)} + \| B_2(v_2 - u_2^h) \|_{L^2(\Omega)}),
\end{aligned}$$

https://doi.org/10.4208/nmtma.2015.w11si Published online by Cambridge University Press

which implies the assertion. □

Now, we introduce the nodal representation. The discretized solution (u_1^h, u_2^h) of (P_h) can be written as follows

$$u_1^h = \sum_{i=1}^{n-1} \xi_i e_i \quad \text{with} \quad \xi_i = B_1 u_1^h(t_i),$$
$$u_2^h = \sum_{i=1}^{n-1} \eta_i e_i \quad \text{with} \quad \eta_i = B_2 u_2^h(t_i).$$

The interpolate (v_1, v_2) of the optimal solution $(\bar{u}_1, \bar{u}_2)$ of (2.1) is as follows

$$v_1 = \sum_{i=1}^{n-1} \phi_i e_i \quad \text{with} \quad \phi_i = B_1 \bar{u}_1(t_i),$$
$$v_2 = \sum_{i=1}^{n-1} \psi_i e_i \quad \text{with} \quad \psi_i = B_2 \bar{u}_2(t_i).$$

Let us recall the adjoint states $(\bar{p}_1, \bar{p}_2)$ defined as

$$\bar{p}_1 := S^*(S(B_1\bar{u}_1 + B_2\bar{u}_2) - z_1),$$
$$\bar{p}_2 := S^*(S(B_1\bar{u}_1 + B_2\bar{u}_2) - z_2).$$

can be represented as interpolations

$$\bar{p}_1 = \sum_{i=1}^{n-1} \mu_i e_i + \delta_{p_1} \quad \text{with} \quad \mu_i = \bar{p}_1(t_i)$$
$$\bar{p}_2 = \sum_{i=1}^{n-1} \rho_i e_i + \delta_{p_2} \quad \text{with} \quad \rho_i = \bar{p}_2(t_i)$$

Remark 3.1. *δ_{p_1} and δ_{p_2} can be estimated under the Assumption* 3.2 *similar to* (3.7) *as follows*

$$\| \delta_{p_1} \|_{L^2(\Omega)} \leq c_5 \cdot h^{3/2}, \tag{3.9}$$

$$\| \delta_{p_2} \|_{L^2(\Omega)} \leq c_6 \cdot h^{3/2}. \tag{3.10}$$

We also define the matrix G, also known as mass matrix -the scalar products of the all basis functions, as follows

$$G = \begin{pmatrix} (e_1, e_1) & \cdots & (e_{N-1}, e_1) \\ \vdots & \ddots & \vdots \\ (e_1, e_{N-1}) & & (e_{N-1}, e_{N-1}) \end{pmatrix}.$$

https://doi.org/10.4208/nmtma.2015.w11si Published online by Cambridge University Press

For our choice of e_i, we have

$$G = \frac{h}{6} \cdot \begin{pmatrix} 2 & 1 & & & 0 \\ 1 & 4 & 1 & & \\ & \ddots & \ddots & \ddots & \\ & & 1 & 4 & 1 \\ 0 & & & 1 & 2 \end{pmatrix}. \tag{3.11}$$

Remark 3.2. The scalar product in $\Omega_h \subset \Omega$ can be expressed by a scalar product in $\mathbb{R}^{n-1}$ using the matrix G. For example, in case of $u_1^h = \sum_{i=1}^{n-1} \xi_i e_i$, we have

$$\| u_1^h \|^2_{L^2(\Omega)} = (u_1^h, u_1^h)_{L^2(\Omega)} = (G\xi, \xi)_{\mathbb{R}^{n-1}}.$$

Remark 3.3. Using the Gershgorin disc, we have the following estimated:

$$\frac{1}{6} h \| \xi \|^2_{\mathbb{R}^{n-1}} \leq (G\xi, \xi)_{\mathbb{R}^{n-1}} = \| u_1^h \|^2_{L^2(\Omega)}$$

This implies

$$\| \xi \|_{\mathbb{R}^{n-1}} \leq \sqrt{\frac{6}{h}} \| u_1^h \|_{L^2(\Omega)}. \tag{3.12}$$

Lemma 3.3. *Under the Assumptions* 3.1 *and* 3.2 *the following estimate holds*

$$\begin{aligned} &(G(\mu + \nu_1 \xi), \phi - \xi)_{\mathbb{R}^{n-1}} + (G(\rho + \nu_2 \eta), \psi - \eta)_{\mathbb{R}^{n-1}} \\ &+ c_7 h^{3/2} (\| B_1(v_1 - u_1^h) \|_{L^2(\Omega)} + \| B_2(v_2 - u_2^h) \|_{L^2(\Omega)}) \geq 0, \end{aligned} \tag{3.13}$$

with $c_7 = c_4 + c_5 + c_6$.

Proof. We can write the inequality (3.8) in the following form

$$\begin{aligned} &(G(\mu + \nu_1 \xi), \phi - \xi)_{\mathbb{R}^{n-1}} + (G(\rho + \nu_2 \eta), \psi - \eta)_{\mathbb{R}^{n-1}} + (\delta_{p1}, v_1 - u_1^h)_{L^2(\Omega)} \\ &+ (\delta_{p2}, v_2 - u_2^h)_{L^2(\Omega)} + c_4 h^{3/2} (\| B_1(v_1 - u_1^h) \|_{L^2(\Omega)} + \| B_2(v_2 - u_2^h) \|_{L^2(\Omega)}) \geq 0. \end{aligned}$$

Now, Remark 3.1 implies

$$\begin{aligned} &(G(\mu + \nu_1 \xi), \phi - \xi)_{\mathbb{R}^{n-1}} + (G(\rho + \nu_2 \eta), \psi - \eta)_{\mathbb{R}^{n-1}} \\ &+ (c_4 + c_5 + c_6) h^{3/2} (\| B_1(v_1 - u_1^h) \|_{L^2(\Omega)} + \| B_2(v_2 - u_2^h) \|_{L^2(\Omega)}) \geq 0. \end{aligned}$$

This completes the proof of the lemma. □

Lemma 3.4. *For* $D \in \mathbb{R}^{(n-1)\times(n-1)}$*, a diagonal matrix with positive entries* d_i*, if the Assumptions* 3.1 *and* 3.2 *hold, we have the following estimates .*

$$(D(\mu + \nu_1 \phi), \xi - \phi)_{\mathbb{R}^{n-1}} \geq 0, \tag{3.14}$$

$$(D(\rho + \nu_2 \psi), \eta - \psi)_{\mathbb{R}^{n-1}} \geq 0. \tag{3.15}$$

https://doi.org/10.4208/nmtma.2015.w11si Published online by Cambridge University Press

Now, we choose a suitable diagonal matrix D as follows

$$D = \frac{h}{6} \cdot \begin{pmatrix} 3 & & & & 0 \\ & 6 & & & \\ & & \ddots & & \\ & & & 6 & \\ 0 & & & & 3 \end{pmatrix}. \tag{3.16}$$

For this particular choice of D, we have

$$G - D = \frac{h}{6} \cdot \begin{pmatrix} -1 & 1 & & & 0 \\ 1 & -2 & 1 & & \\ & \ddots & \ddots & \ddots & \\ & & 1 & -2 & 1 \\ 0 & & & 1 & -1 \end{pmatrix}. \tag{3.17}$$

Lemma 3.5. *If Assumptions* 3.1 *and* 3.2 *are satisfied the following estimates*

$$\| (G-D)\phi \|_{\mathbb{R}^{n-1}} \leq c_8 h^2, \quad \| (G-D)\psi \|_{\mathbb{R}^{n-1}} \leq c_9 h^2, \tag{3.18}$$

$$\| (G-D)\mu \|_{\mathbb{R}^{n-1}} \leq c_{10} h^2, \quad \| (G-D)\rho \|_{\mathbb{R}^{n-1}} \leq c_{11} h^2, \tag{3.19}$$

hold true.

The proofs of the Lemma 3.4 and Lemma 3.5 can be found in [16].

Lemma 3.6. *From Remark* (3.3) *and Lemma* (3.5) *we have the following estimate*

$$\begin{aligned} &((G-D)\phi, \phi - \xi)_{\mathbb{R}^{n-1}} \\ &\leq c_8 h^2 \| \phi - \xi \|_{\mathbb{R}^{n-1}} \leq c_8 \sqrt{6} h^{3/2} \| B_1(v_1 - u_1^h) \|_{L^2(\Omega)} \end{aligned} \tag{3.20}$$

and

$$((G-D)\psi, \psi - \eta)_{\mathbb{R}^{n-1}} \leq c_9 \sqrt{6} h^{3/2} \| B_2(v_2 - u_2^h) \|_{L^2(\Omega)} \tag{3.21}$$

$$((G-D)\mu, \phi - \xi)_{\mathbb{R}^{n-1}} \leq c_{10} \sqrt{6} h^{3/2} \| B_1(v_1 - u_1^h) \|_{L^2(\Omega)} \tag{3.22}$$

$$((G-D)\rho, \psi - \eta)_{\mathbb{R}^{n-1}} \leq c_{11} \sqrt{6} h^{3/2} \| B_2(v_2 - u_2^h) \|_{L^2(\Omega)}. \tag{3.23}$$

hold true.

Now, we are ready to prove the following theorem.

Theorem 3.1. *Assume that the optimal controls $\bar{u}_1, \bar{u}_2$ of the problem* (2.1) *and the corresponding adjoint variables $\bar{p}_1, \bar{p}_2$ satisfy the Assumptions* 3.1 *and* 3.2. *Then the optimal controls (u_1^h, u_2^h), that solve problem (P_h), satisfy the following estimate*

$$\| B_1(\bar{u}_1 - u_1^h) \|_{L^2(\Omega)} + \| B_2(\bar{u}_2 - u_2^h) \|_{L^2(\Omega)} \leq c h^{3/2}. \tag{3.24}$$

https://doi.org/10.4208/nmtma.2015.w11si Published online by Cambridge University Press

Proof. We add the inequalities (3.13), (3.14) and (3.15) to get

$$(G(\mu+\nu_1\xi),\phi-\xi)_{\mathbb{R}^{n-1}}+(G(\rho+\nu_2\eta),\psi-\eta)_{\mathbb{R}^{n-1}}-(D(\mu+\nu_1\phi),\phi-\xi)_{\mathbb{R}^{n-1}}$$
$$-(D(\rho+\nu_2\psi),\psi-\eta)_{\mathbb{R}^{n-1}}+c_7h^{3/2}(\parallel B_1(v_1-u_1^h)\parallel_{L^2(\Omega)}+\parallel B_2(v_2-u_2^h)\parallel_{L^2(\Omega)})\geq 0.$$

This inequality can be written in the form

$$\begin{aligned}&((G-D)\mu,\phi-\xi)_{\mathbb{R}^{n-1}}+((G-D)\rho,\psi-\eta)_{\mathbb{R}^{n-1}}\\&+\nu_1((G-D)\phi,\phi-\xi)_{\mathbb{R}^{n-1}}+\nu_2((G-D)\psi,\psi-\eta)_{\mathbb{R}^{n-1}}\\&+\nu_1(G(\xi-\phi),\phi-\xi)_{\mathbb{R}^{n-1}}+\nu_2(G(\eta-\psi),\psi-\eta)_{\mathbb{R}^{n-1}}\\&+c_7h^{3/2}\Big(\parallel B_1(v_1-u_1^h)\parallel_{L^2(\Omega)}+\parallel B_2(v_2-u_2^h)\parallel_{L^2(\Omega)}\Big)\geq 0.\end{aligned}\tag{3.25}$$

We have

$$\begin{aligned}\nu_1(G(\xi-\phi),\phi-\xi)_{\mathbb{R}^{n-1}}&=-\nu_1\parallel B_1(v_1-u_1^h)\parallel^2_{L^2(\Omega)},\\ \nu_2(G(\eta-\psi),\psi-\eta)_{\mathbb{R}^{n-1}}&=-\nu_2\parallel B_2(v_2-u_2^h)\parallel^2_{L^2(\Omega)}.\end{aligned}$$

With this result and the inequalities from Lemma 3.6, we have

$$\begin{aligned}&\nu_1\parallel B_1(v_1-u_1^h)\parallel^2_{L^2(\Omega)}+\nu_2\parallel B_2(v_2-u_2^h)\parallel^2_{L^2(\Omega)}\\&\leq(c_8+\nu_1c_{10})\sqrt{6}h^{3/2}\parallel B_1(v_1-u_1^h)\parallel_{L^2(\Omega)}+(c_9+\nu_2c_{11})\sqrt{6}h^{3/2}\parallel B_2(v_2-u_2^h)\parallel_{L^2(\Omega)}.\end{aligned}$$

With

$$c_{12}:=\frac{2\sqrt{6}\max(c_8+\nu_1c_{10},c_9+\nu_2c_{11})}{\min(\nu_1,\nu_2)}$$

we have

$$\begin{aligned}&2\parallel B_1(v_1-u_1^h)\parallel^2_{L^2(\Omega)}+2\parallel B_2(v_2-u_2^h)\parallel^2_{L^2(\Omega)})\\&\leq c_{12}h^{3/2}\Big(\parallel B_1(v_1-u_1^h)\parallel_{L^2(\Omega)}+\parallel B_2(v_2-u_2^h)\parallel_{L^2(\Omega)}\Big).\end{aligned}$$

Since

$$\begin{aligned}&\Big(\parallel B_1(v_1-u_1^h)\parallel_{L^2(\Omega)}+\parallel B_2(v_2-u_2^h)\parallel_{L^2(\Omega)}\Big)^2\\&\leq 2\parallel B_1(v_1-u_1^h)\parallel^2_{L^2(\Omega)}+2\parallel B_2(v_2-u_2^h)\parallel^2_{L^2(\Omega)}\end{aligned}\tag{3.26}$$

holds, we have the estimate

$$\parallel B_1(v_1-u_1^h)\parallel_{L^2(\Omega)}+\parallel B_2(v_2-u_2^h)\parallel_{L^2(\Omega)}\leq c_{12}h^{3/2}.\tag{3.27}$$

https://doi.org/10.4208/nmtma.2015.w11si Published online by Cambridge University Press

Now using (3.7) and (3.27), we obtain

$$\begin{aligned}
&\| B_1(\bar{u}_1 - u_1^h) \|_{L^2(\Omega)} + \| B_2(\bar{u}_2 - u_2^h) \|_{L^2(\Omega)} \\
\leq &\| B_1(\bar{u}_1 - v_1) \|_{L^2(\Omega)} + \| B_2(\bar{u}_2 - v_2) \|_{L^2(\Omega)} \\
&+ \| B_1(v_1 - u_1^h) \|_{L^2(\Omega)} + \| B_2(v_2 - u_2^h) \|_{L^2(\Omega)} \\
\leq &(c_1 + c_2 + c_{12}) h^{3/2} = c\, h^{3/2}.
\end{aligned}$$

Thus for a positive constant $c = (c_1 + c_2 + c_{12})$, we have proved the theorem. □

Similar estimate of order $h^{3/2}$ can be proved for the state as well. On the other hand, the estimates are difficult to verify by numerical experiments for the PDE-constraints of second order, if the adjoints and the controls are restricted to the assumptions 3.1 and 3.2. Analytical solution can be found for more regular adjoints and controls which makes the numerical verification easier. But due to the increased regularity, the order of approximation for state and controls can be observed of order h^2. In Section 6, we present numerical experiments where h^2 convergence is evident for both state and controls.

4. A FEM-multigrid scheme

In order to solve efficiently our multi-objective optimality system, we discuss in this section a multigrid scheme for elliptic Nash-equilibrium optimal control problems with control constraints. Multigrid methods are iterative methods that use a hierarchy of discretization spaces [5]. Two complementary solution strategies are employed to efficiently reduce the high- and low-frequency error components of the solution. For the high-frequency error components, a smoothing algorithm is used, while for the low-frequency error components a coarse-grid correction strategy is utilized. This turns out to be an efficient strategy as the high-frequency errors are reduced quite fast under smoothing operation. Whereas the low-frequency errors appear as high-frequency error in the coarser grid, enabling to reduce them efficiently by smoothing in the coarse grid.

We use the nonlinear full approximation storage (FAS) framework with full multigrid (FMG) cycle [4]. The FAS scheme allows to accommodate non-linearities like the inequalities representing the optimality conditions. The FAS scheme is illustrated in the following.

We denote with the index k the operators and variables defined on the uniform triangulation with representative mesh size $h = h_k = h_0/2^k, k = 1, \ldots, L$, where L denotes the finest level. Let us consider the optimality system (3.6) at the discretization level k for the unknown variables $\Phi_k = (y_k, u_{1,k}, u_{2,k}, p_{1,k}, p_{2,k})$. We write the optimality system in a compact notation as follows

$$A_k(\Phi_k) = F_k, \tag{4.1}$$

where $A_k(\cdot)$ represents the discrete nonlinear optimality system on grid level k.

https://doi.org/10.4208/nmtma.2015.w11si Published online by Cambridge University Press

We denote the result of our smoothing scheme with $\Phi_k^{(l)} = S_k(\Phi_k^{(l-1)}, F_k)$. Suppose to apply m_1-times this iteration to (4.1) starting with the approximation $\Phi_k^{(0)}$ to obtain the approximate solution $\tilde{\Phi}_k = \Phi_k^{(m_1)}$.

In our nonlinear setting the desired correction e_k to $\tilde{\Phi}_k$ is defined by $A_k(\tilde{\Phi}_k + e_k) = F_k$. We define this correction as the solution to

$$A_k(\tilde{\Phi}_k + e_k) - A_k(\tilde{\Phi}_k) = r_k \tag{4.2}$$

where $r_k = F_k - A_k(\tilde{\Phi}_k)$ is the residual associated to $\tilde{\Phi}_k$.

In order to represent $\tilde{\Phi}_k + e_k$ on the coarse grid, we write

$$\Phi_{k-1} := I_k^{k-1}\tilde{\Phi}_k + e_{k-1}. \tag{4.3}$$

where Φ_{k-1} represents the solution in the coarse grid. The linear operator I_k^{k-1} is chosen as injection operator. As e_k is smooth due to the action of S_k, we may represent e_k by a coarse function e_{k-1}.

In order to formulate (4.2) on the coarse grid, we replace $A_k(\cdot)$ by $A_{k-1}(\cdot)$, $\tilde{\Phi}_k$ by $I_k^{k-1}\tilde{\Phi}_k$, and r_k by restriction $r_{k-1} = I_k^{k-1}r_k = I_k^{k-1}(F_k - A_k(\tilde{\Phi}_k))$. We get the following (FAS) equation

$$A_{k-1}(\Phi_{k-1}) = I_k^{k-1}(F_k - A_k(\tilde{\Phi}_k)) + A_{k-1}(I_k^{k-1}\tilde{\Phi}_k). \tag{4.4}$$

With

$$\tau_k^{k-1} = A_{k-1}(I_k^{k-1}\tilde{\Phi}_k) - I_k^{k-1}A_k(\tilde{\Phi}_k),$$

(4.4) can also be written in the form $A_{k-1}(\Phi_{k-1}) = I_k^{k-1}F_k + \tau_k^{k-1}$.

The term τ_k^{k-1} is a fine-to-coarse defect or residual correction such that at convergence the solution to (4.4) coincides with the fine grid solution in the sense that $\Phi_{k-1} = I_k^{k-1}\Phi_k$. The solution to (4.4) provides Φ_{k-1}. From (4.3) we have

$$e_{k-1} = \Phi_{k-1} - I_k^{k-1}\tilde{\Phi}_k. \tag{4.5}$$

Therefore we can obtain a coarse-grid correction to the fine-grid approximation as follows

$$\Phi_k = \tilde{\Phi}_k + I_{k-1}^k(\Phi_{k-1} - I_k^{k-1}\tilde{\Phi}_k). \tag{4.6}$$

Here, I_{k-1}^k is the coarse-to-fine interpolation operator. In order to damp possible high-frequency errors arising through the entire coarse-grid correction process, the correction step (4.6) is followed by m_2-times smoothing iteration. The FAS cycle is summarized in the following algorithm.

https://doi.org/10.4208/nmtma.2015.w11si Published online by Cambridge University Press

Algorithm 4.1. ***FAS*** (m_1, m_2) ***for solving*** $A_k(\Phi_k) = F_k$ ***starting with*** Φ_k^0**.**

1. If $k = 1$solve $A_k(\Phi_k) = F_k$ exactly.
2. Pre-smoothing steps on the fine grid: $\Phi_k^{(l)} = S_k(\Phi_k^{(l-1)}, F_k), l = 1, \ldots, m_1$;
3. Computation of the residual: $r_k = F_k - A_k(\Phi_k^{(m_1)})$;
4. Restriction of the residual: $r_{k-1} = I_k^{k-1} r_k$;
5. Set $\Phi_{k-1} = I_k^{k-1} \Phi_k^{(m_1)}$;
6. Set $F_{k-1} = r_{k-1} + A_{k-1}(\Phi_{k-1})$;
7. Call γ times FAS (m_1, m_2) to solve $A_{k-1}(\Phi_{k-1}) = F_{k-1}$;
8. Coarse-grid correction: $\Phi^{(m_1+1)} = \Phi_k^{(m_1)} + I_{k-1}^k(\Phi_{k-1} - I_k^{k-1}\Phi_k^{(m_1)})$;
9. Post-smoothing steps on the final grid: $\Phi_k^{(l)} = S_k(\Phi_k^{(l-1)}, F_k), l = m_1 + 2, \ldots, m_1 + m_2 + 1$;

We can perform γ two-grid iterations at each working level. For $\gamma = 1$ we have a V-cycle and for $\gamma = 2$ we have a W-cycle.

To start the iterative procedure from a good initial approximation, we employ the so called full multigrid method (FMG). Suppose to start the solution process from a coarse working level $K < M$ where the discretized problem $A_l(\Phi_l) = F_l$ with $l = K$ is easily solved. The idea is to interpolate this solution to the next finer working level as initial approximation for the iterative process to solve $A_{l+1}(\Phi_{l+1}) = F_{l+1}$ as $\Phi_{l+1} = I_l^{l+1}\Phi_l$. Thereafter the FAS solution process at level $l + 1$ is applied. The idea of using a coarse grid approximation as a first guess for the solution process on a finer grid is known as nested iteration. As better starting solutions at each starting level are available, the scheme results to be more efficient and of optimal computational complexity than the iterative application of the multigrid cycle without FMG initialization [5]. A description of the FMG method is given in the following algorithm.

Algorithm 4.2. ***FMG-cycle for solving*** $A_L(\Phi_L) = F_L$**.**

1. For $l = K < L$ set initial approximation u_l.
2. If $l < L$ then interpolate to the next finer working level: $\tilde{\Phi}_{l+1} = I_l^{l+1}\Phi_l$;
3. Apply FAS μ times to solve $A_{l+1}(\Phi_{l+1}) = F_{l+1}$, starting with $\tilde{\Phi}_{l+1}$;
4. Set $l := l + 1$. If $l < L$ go to 2; else stop.

https://doi.org/10.4208/nmtma.2015.w11si Published online by Cambridge University Press

Based on previous experience [3], We develop a collective smoothing step to update the controls, the state and the adjoint variables lexicographically on each nodal point. From the discretized optimality system, we obtain the following equations for a ith nodal point. We have

$$Y_i = \frac{1}{K_{i,i}}\Big(-\sum_{\substack{j=0\\ j\neq i}}^{n} K_{i,j}Y_j + \sum_{\substack{j=0\\ j\neq i}}^{n} M_{i,j}U_j + M_{i,i}U_i\Big), \tag{4.7a}$$

$$P_{1,i} = \frac{1}{K_{i,i}}[Z_{1,i} - \sum_{\substack{j=0\\ j\neq i}}^{n} K_{i,j}P_{1,j} + \sum_{\substack{j=0\\ j\neq i}}^{n} M_{i,j}Y_j + M_{i,i}Y_i\Big), \tag{4.7b}$$

$$P_{2,i} = \frac{1}{K_{i,i}}[Z_{2,i} - \sum_{\substack{j=0\\ j\neq i}}^{n} K_{i,j}P_{2,j} + \sum_{\substack{j=0\\ j\neq i}}^{n} M_{i,j}Y_j + M_{i,i}Y_i\Big) \tag{4.7c}$$

$$U_i = \begin{cases} U_{1,i} = \min\{b_1, \max\{a_1, -\dfrac{P_{1,i}}{\nu_1}\}\} & \forall\, U_i \in \omega_1 \\ U_{2,i} = \min\{b_2, \max\{a_2, -\dfrac{P_{2,i}}{\nu_2}\}\} & \forall\, U_i \in \omega_2 \\ 0 & \text{otherwise.} \end{cases} \tag{4.7d}$$

Let us define $\tilde{U}_{1,i} := -P_{1,i}/\nu_1$ and $\tilde{U}_{2,i} := -P_{2,i}/\nu_2$. We combine the state and adjoint equations with the optimality condition to compute the updates for $\tilde{U}_{1,i}$ and $\tilde{U}_{2,i}$ with

$$C_1 = \sum_{\substack{j=0\\ j\neq i}}^{n} M_{i,j}Y_j \qquad C_2 = \sum_{\substack{j=0\\ j\neq i}}^{n} K_{i,j}Y_j, \tag{4.8a}$$

$$C_3 = \sum_{\substack{j=0\\ j\neq i}}^{n} K_{i,j}P_{1,j} \qquad C_4 = \sum_{\substack{j=0\\ j\neq i}}^{n} K_{i,j}P_{2,j}, \qquad C_5 = \sum_{\substack{j=0\\ j\neq i}}^{n} M_{i,j}U_j, \tag{4.8b}$$

$$\tilde{U}_{1,i} = \frac{1}{\nu_1 + \dfrac{M_{i,i}^2}{K_{i,i}^2}}\Big(\frac{1}{K_{i,i}}(C_1 - Z_{1,i} - C_3) + \frac{M_{i,i}}{K_{i,i}^2}(C_5 - C_2)\Big), \tag{4.8c}$$

$$\tilde{U}_{2,i} = \frac{1}{\nu_2 + \dfrac{M_{i,i}^2}{K_{i,i}^2}}\Big(\frac{1}{K_{i,i}}(C_1 - Z_{2,i} - C_4) + \frac{M_{i,i}}{K_{i,i}^2}(C_5 - C_2)\Big). \tag{4.8d}$$

We update $U_{1,i}$ $U_{2,i}$ as follows

$$U_{1,i} = \begin{cases} a_1 & \text{if } \tilde{U}_{1,i} < a_1, \\ \tilde{U}_{1,i} & \text{if } a_1 \le \tilde{U}_{1,i} \le b_1, \\ b_1 & \text{if } \tilde{U}_{1,i} > b_1, \end{cases} \qquad U_{2,i} = \begin{cases} a_2 & \text{if } \tilde{U}_{2,i} < a_2, \\ \tilde{U}_{2,i} & \text{if } a_2 \le \tilde{U}_{2,i} \le b_2, \\ b_2 & \text{if } \tilde{U}_{2,i} > b_2, \end{cases} \tag{4.9}$$

https://doi.org/10.4208/nmtma.2015.w11si Published online by Cambridge University Press

which is followed by the update of the state and the adjoint variables

$$U_i = \begin{cases} U_{1,i} & \text{if} \quad U_i \in \omega_1 \\ U_{2,i} & \text{if} \quad U_i \in \omega_2 \\ 0 & \text{otherwise} \end{cases} \tag{4.10a}$$

$$Y_i = \frac{1}{K_{i,i}}[-C_2 + C_5 + M_{i,i}U_i] \tag{4.10b}$$

$$P_{1,i} = \frac{1}{K_{i,i}}[Z_{1,i} - C_3 + C_1 + M_{i,i}Y_i] \tag{4.10c}$$

$$P_{2,i} = \frac{1}{K_{i,i}}[Z_{2,i} - C_4 + C_1 + M_{i,i}Y_i]. \tag{4.10d}$$

One smoothing step consists in applying the procedures (4.9)-(4.10) lexicographically to all nodal points.

We complete this section describing the restriction and the prolongation operators. Between two grids corresponding to the mesh size h_k and coarse mesh h_{k-1}, we apply the 7-point prolongation operator $I_{k-1}^k : L_{k-1}^2 \to L_k^2$, given in stencil form by

$$I_{k-1}^k = \frac{1}{2}\begin{bmatrix} & 1 & 1 \\ 1 & 2 & 1 \\ 1 & 1 & \end{bmatrix}. \tag{4.11}$$

For restricting the residuals, we use the following restriction operator, $I_k^{k-1} : L_k^2 \to L_{k-1}^2$, given by the stencil

$$I_k^{k-1} = \frac{1}{8}\begin{bmatrix} & 1 & 1 \\ 1 & 2 & 1 \\ 1 & 1 & \end{bmatrix}. \tag{4.12}$$

5. Local Fourier analysis

We present a local Fourier analysis to investigate the convergence properties of the proposed multigrid scheme. We assume an unconstrained problem on a regular grid. At first, we investigate the smoothing iteration and then we present a two grid analysis.

We proceed with Eq. (3.6) by replacing the control variables with the corresponding adjoint variables as no constraints are assumed to be active. We have

$$U_1 = -\frac{P_1}{\nu_1} \qquad \text{and} \qquad U_2 = -\frac{P_2}{\nu_2}.$$

This leads us to the following optimality system.

$$\begin{array}{llll} KY & + MB_1\dfrac{P_1}{\nu_1} & + MB_2\dfrac{P_2}{\nu_2} & = \mathbf{0}, \\ -MY & + KP_1 & & = -Z_1, \\ -MY & & + KP_2 & = -Z_2. \end{array} \tag{5.1}$$

https://doi.org/10.4208/nmtma.2015.w11si Published online by Cambridge University Press

For a regular grid with linear triangular elements, the stiffness matrix and the mass matrix result in the following stencils

$$K_h = \begin{bmatrix} & -1 & \\ -1 & 4 & -1 \\ & -1 & \end{bmatrix} \quad \text{and} \quad M_h = \frac{4h^2}{3}\begin{bmatrix} & 1 & 1 \\ 1 & 6 & 1 \\ 1 & 1 & \end{bmatrix}. \tag{5.2}$$

Now, we consider the splitting for these two operators as follows

$$K_h^+ = \begin{bmatrix} & 0 & \\ -1 & 4 & 0 \\ & -1 & \end{bmatrix}, \qquad K_h^- = \begin{bmatrix} & -1 & \\ 0 & 0 & -1 \\ & 0 & \end{bmatrix},$$
$$M_h^+ = \frac{4h^2}{3}\begin{bmatrix} & 0 & 0 \\ 1 & 6 & 0 \\ 1 & 1 & \end{bmatrix}, \qquad M_h^- = \frac{4h^2}{3}\begin{bmatrix} & 1 & 1 \\ 0 & 0 & 1 \\ 0 & 0 & \end{bmatrix}.$$

We recall the local Fourier setting. We consider a sequence of triangulations, $\Omega_k = \{(ih_k, jh_k), i, j \in \mathbb{Z}\}$ where we define the Fourier components:

$$\phi(\boldsymbol{\theta}, \mathbf{x}) := e^{i\boldsymbol{\theta}\cdot\mathbf{x}/\mathbf{h}} = e^{i\theta_1 x_1/h_k} e^{i\theta_2 x_2/h_k}$$

We have the following

- Low-frequency components of ϕ: $\boldsymbol{\theta} = (\theta_1, \theta_2) \in [-\pi/2, \pi/2)^2$;
- High-frequency components of ϕ: $\boldsymbol{\theta} = (\theta_1, \theta_2) \in [-\pi, \pi)^2 \backslash [-\pi/2, \pi/2)^2$.

Corresponding to a low-frequency component, we consider the following harmonics

$$\boldsymbol{\theta}^{(0,0)} := (\theta_1, \theta_2), \qquad \boldsymbol{\theta}^{(1,1)} := (\bar{\theta}_1, \bar{\theta}_2),$$
$$\boldsymbol{\theta}^{(1,0)} := (\bar{\theta}_1, \theta_2), \qquad \boldsymbol{\theta}^{(0,1)} := (\theta_1, \bar{\theta}_2),$$

where

$$\bar{\theta}_i = \begin{cases} \theta_i + \pi & \text{if} \quad \theta_i < 0, \\ \theta_i - \pi & \text{if} \quad \theta_i \geq 0. \end{cases}$$

With this notation, θ represents the low frequency components and $\bar{\theta}$ represents the high frequency components. We also denote with $\boldsymbol{\alpha} = (\alpha_1, \alpha_2) \in \{(0,0), (1,1), (1,0), (0,1)\}$. In order to investigate the smoothing properties, we define the error functions (e_y, e_{p_1}, e_{p_2}) for y_h, p_{1h} and p_{2h} as follows

$$e_y(\mathbf{x}) = \sum_{\boldsymbol{\alpha},\boldsymbol{\theta}} Y_{\boldsymbol{\alpha},\boldsymbol{\theta}} \phi(\boldsymbol{\theta}^{\boldsymbol{\alpha}}, \mathbf{x}), \quad e_{p_1}(\mathbf{x}) = \sum_{\boldsymbol{\alpha},\boldsymbol{\theta}} P1_{\,\boldsymbol{\alpha},\boldsymbol{\theta}} \phi(\boldsymbol{\theta}^{\boldsymbol{\alpha}}, \mathbf{x}), \quad e_{p_2}(\mathbf{x}) = \sum_{\boldsymbol{\alpha},\boldsymbol{\theta}} P2_{\,\boldsymbol{\alpha},\boldsymbol{\theta}} \phi(\boldsymbol{\theta}^{\boldsymbol{\alpha}}, \mathbf{x}),$$

https://doi.org/10.4208/nmtma.2015.w11si Published online by Cambridge University Press

where $W_{\boldsymbol{\alpha},\boldsymbol{\theta}} = (Y_{\boldsymbol{\alpha},\boldsymbol{\theta}}, P_{1\,\boldsymbol{\alpha},\boldsymbol{\theta}}, P_{2\,\boldsymbol{\alpha},\boldsymbol{\theta}})$ represent the Fourier coefficients of the corresponding functions. We express the reduction of the error due to one smoothing step with the Fourier symbol of the smoothing operator $\hat{S}(\boldsymbol{\alpha},\boldsymbol{\theta})$ as follows

$$W^{(1)}_{\boldsymbol{\alpha},\boldsymbol{\theta}} = \hat{S}(\boldsymbol{\alpha},\boldsymbol{\theta}) W^{(0)}_{\boldsymbol{\alpha},\boldsymbol{\theta}}.$$

Now, we compute the Fourier symbols $\tilde{K}_h^+$, $\tilde{K}_h^-$, $\tilde{M}_h^+$ and $\tilde{M}_h^-$ of the operators K_h^+, K_h^-, M_h^+ and M_h^-.

$$K_h^+ e^{i\boldsymbol{\theta}\cdot\mathbf{x}/\mathbf{h}} = \begin{bmatrix} & 0 & \\ -1 & 4 & 0 \\ & -1 & \end{bmatrix} e^{i\boldsymbol{\theta}\cdot\mathbf{x}/\mathbf{h}} = (4 - e^{i\theta_1} - e^{i\theta_2}) e^{i\boldsymbol{\theta}\cdot\mathbf{x}/\mathbf{h}}$$

Thus

$$\tilde{K}_h^+(\boldsymbol{\theta}) \;\; = \;\; (4 - e^{-i\theta_1} - e^{-i\theta_2}).$$

Similarly,

$$\begin{aligned} \tilde{K}_h^-(\boldsymbol{\theta}) &= -(e^{i\theta_1} + e^{i\theta_2}), \\ \tilde{M}_h^+(\boldsymbol{\theta}) &= \frac{4h^2}{3}(6 + e^{-i\theta_1} + e^{-i\theta_2} + e^{-i(\theta_1+\theta_2)}), \\ \tilde{M}_h^-(\boldsymbol{\theta}) &= \frac{4h^2}{3}(e^{i\theta_1} + e^{i\theta_2} + e^{i(\theta_1+\theta_2)}). \end{aligned}$$

With these Fourier symbols and considering the optimality system (5.1), we compute the Fourier symbol for the smoothing iteration $\hat{S}_k(\boldsymbol{\theta})$ on the triangulation Ω_k as follows

$$\hat{S}_k(\boldsymbol{\theta}) = \begin{bmatrix} \tilde{K}_h^+(\boldsymbol{\theta}) & \frac{B_1}{\nu_1}\tilde{M}_h^+(\boldsymbol{\theta}) & \frac{B_2}{\nu_2}\tilde{M}_h^+(\boldsymbol{\theta}) \\ -\tilde{M}_h^+(\boldsymbol{\theta}) & \tilde{K}_h^+(\boldsymbol{\theta}) & 0 \\ -\tilde{M}_h^+(\boldsymbol{\theta}) & 0 & \tilde{K}_h^+(\boldsymbol{\theta}) \end{bmatrix}^{-1} \times \begin{bmatrix} -\tilde{K}_h^-(\boldsymbol{\theta}) & \frac{-B_1}{\nu_1}\tilde{M}_h^-(\boldsymbol{\theta}) & \frac{-B_2}{\nu_2}\tilde{M}_h^-(\boldsymbol{\theta}) \\ \tilde{M}_h^-(\boldsymbol{\theta}) & -\tilde{K}_h^-(\boldsymbol{\theta}) & 0 \\ \tilde{M}_h^-(\boldsymbol{\theta}) & 0 & -\tilde{K}_h^-(\boldsymbol{\theta}) \end{bmatrix}. \tag{5.3}$$

The smoothing factor of the collective scheme is given by

$$\mu = \mu(S_k) = \sup\{|\rho(\hat{S}_k(\boldsymbol{\theta}))| : \boldsymbol{\theta} \text{ high frequency}\} \tag{5.4}$$

where ρ denotes the spectral radius. The smoothing factor can be computed for any choice of h, ν_1 and ν_2. The values of B_1 and B_2 are either 0 or 1 depending on the sub-domain being considered.

For the two level analysis, we proceed with the coarse-grid correction operator

$$CG_k^{k-1} = [I_k - I_{k-1}^k (A_{k-1})^{-1} I_k^{k-1} A_k],$$

and its corresponding symbol

$$\widehat{CG}_k^{k-1} = [\hat{I}_k - \hat{I}_{k-1}^k(\boldsymbol{\theta})(\widehat{A}_{k-1}(\boldsymbol{\theta}))^{-1} \hat{I}_k^{k-1}(\boldsymbol{\theta}) \widehat{A}_k(\boldsymbol{\theta})].$$

https://doi.org/10.4208/nmtma.2015.w11si Published online by Cambridge University Press

The symbol for the operator of the optimality system at coarse grid A_{k-1} is given by

$$\widehat{A}_{k-1}(\boldsymbol{\theta}) = \begin{bmatrix} a_{k-1,1} & \dfrac{B_1}{\nu_1}a_{k-1,2} & \dfrac{B_2}{\nu_2}a_{k-1,2} \\ -a_{k-1,2} & a_{k-1,1} & 0 \\ -a_{k-1,2} & 0 & a_{k-1,1} \end{bmatrix}. \tag{5.5}$$

with

$$a_{k-1,1} = 4 - 2\cos(2\theta_1) - 2\cos(2\theta_2) \quad \text{and}$$
$$a_{k-1,2} = \frac{4h_{k-1}^2}{3}[6 + 2\cos(2\theta_1) + 2\cos(2\theta_2) + 2\cos(2\theta_1 + 2\theta_2)].$$

Similarly, we have for the operator of the optimality system at the fine grid

$$\widehat{A}_k(\boldsymbol{\theta}) = \begin{bmatrix} [A_{k,1}] & \dfrac{B_1}{\nu_1}[A_{k,2}] & \dfrac{B_2}{\nu_2}[A_{k,2}] \\ -[A_{k,2}] & [A_{k,1}] & [\mathbf{0}] \\ -[A_{k,2}] & [\mathbf{0}] & [A_{k,1}] \end{bmatrix} \tag{5.6}$$

where

$$A_{k,1} = \begin{bmatrix} l_1(\boldsymbol{\theta}^{(0,0)}) & 0 & 0 & 0 \\ 0 & l_1(\boldsymbol{\theta}^{(1,1)}) & 0 & 0 \\ 0 & 0 & l_1(\boldsymbol{\theta}^{(1,0)}) & 0 \\ 0 & 0 & 0 & l_1(\boldsymbol{\theta}^{(0,0)}) \end{bmatrix},$$

$$A_{k,2} = \begin{bmatrix} l_2(\boldsymbol{\theta}^{(0,0)}) & 0 & 0 & 0 \\ 0 & l_2(\boldsymbol{\theta}^{(1,1)}) & 0 & 0 \\ 0 & 0 & l_2(\boldsymbol{\theta}^{(1,0)}) & 0 \\ 0 & 0 & 0 & l_2(\boldsymbol{\theta}^{(0,1)}) \end{bmatrix},$$

$$l_1(\boldsymbol{\theta}^{\boldsymbol{\alpha}}) = 4 - 2(\cos(\theta_1^{\alpha_1}) + \cos(\theta_2^{\alpha_2})),$$

and

$$l_2(\boldsymbol{\theta}^{\boldsymbol{\alpha}}) = \frac{4h_k^2}{3}[6 + 2(\cos(\theta_1^{\alpha_1}) + \cos(\theta_2^{\alpha_2}) + \cos(\theta_1^{\alpha_1} + \theta_2^{\alpha_2}))\,].$$

The Fourier symbol for the restriction operator is given by

$$\hat{I}_k^{k-1}(\boldsymbol{\theta}) = \begin{bmatrix} [I_1] & & \\ & [I_1] & \\ & & [I_1] \end{bmatrix} \tag{5.7}$$

where

$$I_1 = \begin{bmatrix} I(\boldsymbol{\theta}^{(0,0)}) & I(\boldsymbol{\theta}^{(1,1)}) & I(\boldsymbol{\theta}^{(1,0)}) & I(\boldsymbol{\theta}^{(0,1)}) \end{bmatrix},$$

https://doi.org/10.4208/nmtma.2015.w11si Published online by Cambridge University Press

and

$$I(\boldsymbol{\theta}^{\boldsymbol{\alpha}}) = \frac{1}{4}[1 + \cos(\theta_1^{\alpha_1}) + \cos(\theta_2^{\alpha_2}) + \cos(\theta_1^{\alpha_1} + \theta_2^{\alpha_2})].$$

For the prolongation operator, we have

$$\hat{I}_{k-1}^{k}(\boldsymbol{\theta}) = 4 \cdot \hat{I}_{k}^{k-1}(\boldsymbol{\theta})^{T}. \tag{5.8}$$

Finally, the symbol for the twolevel method is given by

$$\widehat{TG}_k^{k-1}(\boldsymbol{\theta}) = \hat{S}_k^{\nu_1}(\boldsymbol{\theta})\widehat{CG}_k^{k-1}(\boldsymbol{\theta})\hat{S}_k^{\nu_2}(\boldsymbol{\theta}). \tag{5.9}$$

The convergence factor is defined as follows

$$\eta = \eta(TG_k^{k-1}) = \sup\{|\rho(\widehat{TG}_k^{k-1}(\boldsymbol{\theta}))| : \boldsymbol{\theta} \in [-\pi/2, \pi/2)^2\}. \tag{5.10}$$

Numerical smoothing and convergence factor estimates given by (5.4) and (5.10) are reported in the next section.

6. Numerical Experiments

In this section, we present results of numerical experiments to validate the effectiveness of the proposed scheme. We consider problems on a two-dimensional domain discretized with linear triangular elements. First, we discuss the accuracy of the FEM solution. Then we show the tracking property of the scheme and at last we investigate the multigrid convergence properties. In all of these experiments, we considered both constrained- and unconstrained-control cases.

The multigrid setup used for the experiments are as follows. Three pre- and post-smoothing iterations suggested by the local Fourier analysis. But from the numerical experiments (c.f. Table 4) two pre- and post-smoothing operations are found to be sufficient. Next, for the FAS cycle the V-cycle ($\gamma = 1$) is employed. We use two FAS iterations ($\mu = 2$) during initialization of the FMG-cycle. These parameters are chosen based on the experience from the numerical experiments.

First, we show how the computed solution converges as we refine the mesh. To make this comparison, we construct a problem such that we have an analytical solution for the state and the controls.

We define the domains as follows

$$\Omega = (-1, 1) \times (0, 1), \quad \omega_1 = (-1, 0) \times (0, 1) \quad \text{and} \quad \omega_2 = (0, 1) \times (0, 1).$$

We consider the state constraint to be

$$-\Delta y = B_1 u_1 + B_2 u_2 + f.$$

The state is chosen as

$$y := 10(x_1^2 - x_1^4)(x_2 - x_2^2),$$

https://doi.org/10.4208/nmtma.2015.w11si Published online by Cambridge University Press

and the controls are chosen as

$$u_1 := -\sin(\pi x_1)\sin(\pi x_2),$$

$$u_2 := \sin(\pi x_1)\sin(\pi x_2),$$

For the unconstrained case, we consider the control constraints to be

$$0 \le u_j \le 0.7 \quad \text{for } j = 1, 2.$$

The analytical solutions for the controls are given by

$$u_1 := \min(0.7, \max(0, -\sin(\pi x_1)\sin(\pi x_2)))$$

$$u_2 := \min(0.7, \max(0, \sin(\pi x_1)\sin(\pi x_2)))$$

for the control-constrained problem. We choose $\nu_1 = 10^{-1}$ and $\nu_2 = 10^{-2}$. Now, with the analytical solutions at hand, we can compare the results for different meshes for both constrained and unconstrained cases. These results are reported in Table 1.

Table 1: Accuracy

h	$\| y_{ex} - y^h \|_{L^2}$	$\| u_{1\,ex} - u_1^h \|_{L^2}$	
Case 1: Unconstrained case			
1/8	$2.07 \cdot 10^{-2}$	$2.43 \cdot 10^{-1}$	$4.54 \cdot 10^{-2}$
1/16	$5.24 \cdot 10^{-3}$	$6.44 \cdot 10^{-2}$	$1.23 \cdot 10^{-2}$
1/32	$1.31 \cdot 10^{-3}$	$1.64 \cdot 10^{-2}$	$3.14 \cdot 10^{-3}$
1/64	$3.29 \cdot 10^{-4}$	$4.12 \cdot 10^{-3}$	$7.88 \cdot 10^{-4}$
1/128	$8.23 \cdot 10^{-5}$	$1.03 \cdot 10^{-3}$	$1.97 \cdot 10^{-4}$
Case 2: Constrained case			
1/8	$2.31 \cdot 10^{-2}$	$1.54 \cdot 10^{-1}$	$3.04 \cdot 10^{-2}$
1/16	$5.56 \cdot 10^{-3}$	$6.36 \cdot 10^{-2}$	$1.01 \cdot 10^{-2}$
1/32	$1.37 \cdot 10^{-3}$	$1.70 \cdot 10^{-2}$	$2.87 \cdot 10^{-3}$
1/64	$3.43 \cdot 10^{-4}$	$4.32 \cdot 10^{-3}$	$8.25 \cdot 10^{-4}$
1/128	$8.58 \cdot 10^{-5}$	$1.09 \cdot 10^{-3}$	$2.47 \cdot 10^{-4}$

We see at the second column the L^2 error for the state. It is evident that this error is reduced in the order of h^2 with each mesh refinement. In the next two columns the error for the controls are presented. The controls are also found to have quadratic convergence for both cases.

Next, we discuss the optimization properties of the algorithm. In the experiment, we test the tracking ability of our scheme as we take ν_1 and ν_2 smaller, also in the case where these parameters are not equal. As above, we also investigated both constrained and unconstrained cases.

https://doi.org/10.4208/nmtma.2015.w11si Published online by Cambridge University Press

Table 2: Tracking ability without control constraints.

$\| y - z_1 \|^2_{L^2}$	$\| y - z_2 \|^2_{L^2}$	ν_1	ν_2
Case 1: $\nu_1 = \nu_2$			
$89.738 \cdot 10^{-3}$	$89.738 \cdot 10^{-3}$	10^{-1}	10^{-1}
$87.482 \cdot 10^{-3}$	$87.482 \cdot 10^{-3}$	10^{-2}	10^{-2}
$72.317 \cdot 10^{-3}$	$72.317 \cdot 10^{-3}$	10^{-3}	10^{-3}
$59.050 \cdot 10^{-3}$	$59.050 \cdot 10^{-3}$	10^{-4}	10^{-4}
Case 2: Constrained case			
$151.007 \cdot 10^{-3}$	$18.005 \cdot 10^{-3}$	10^{-1}	10^{-6}
$149.409 \cdot 10^{-3}$	$18.133 \cdot 10^{-3}$	10^{-2}	10^{-6}
$136.254 \cdot 10^{-3}$	$20.021 \cdot 10^{-3}$	10^{-3}	10^{-6}
$96.846 \cdot 10^{-3}$	$41.870 \cdot 10^{-3}$	10^{-4}	10^{-6}

Table 3: Tracking ability with control constraints.

$\| y - z_1 \|^2_{L^2}$	$\| y - z_2 \|^2_{L^2}$	ν_1	ν_2
Case 1: $\nu_1 = \nu_2$			
$89.738 \cdot 10^{-3}$	$89.738 \cdot 10^{-3}$	10^{-1}	10^{-1}
$87.482 \cdot 10^{-3}$	$87.482 \cdot 10^{-3}$	10^{-2}	10^{-2}
$72.317 \cdot 10^{-3}$	$72.317 \cdot 10^{-3}$	10^{-3}	10^{-3}
$59.050 \cdot 10^{-3}$	$59.050 \cdot 10^{-3}$	10^{-4}	10^{-4}
Case 2: Constrained case			
$147.880 \cdot 10^{-3}$	$19.870 \cdot 10^{-3}$	10^{-1}	10^{-6}
$146.248 \cdot 10^{-3}$	$20.047 \cdot 10^{-3}$	10^{-2}	10^{-6}
$132.890 \cdot 10^{-3}$	$22.351 \cdot 10^{-3}$	10^{-3}	10^{-6}
$93.521 \cdot 10^{-3}$	$44.592 \cdot 10^{-3}$	10^{-4}	10^{-6}

We chose the domains to be $\Omega = (0,1) \times (0,0.5)$, and

$$\omega_1 = (0.1,0.4) \times (0.1,0.4), \quad \omega_2 = (0.6,0.9) \times (0.1,0.4).$$

And the target functions are defined for $j = 1, 2$, as follows

$$z_j := \begin{cases} 1 & \text{if } (x_1, x_2) \in \omega_j \\ 0 & \text{otherwise} \end{cases}$$

The numerical results are presented in the Tables 2 and 3.

We see clearly from Tables 2 and 3 that for smaller values of ν_1 and ν_2, the states are closer to the target functions. For the different values of the weights, we see that the state is closer to the target function corresponding to the control with the smaller weight. We also observe the same performance in the control-constrained case.

Further, notice in Fig. 1 that the convergence rate of the multigrid scheme does not depend on the values of the weights of the cost of the controls. However, for a fixed

https://doi.org/10.4208/nmtma.2015.w11si Published online by Cambridge University Press

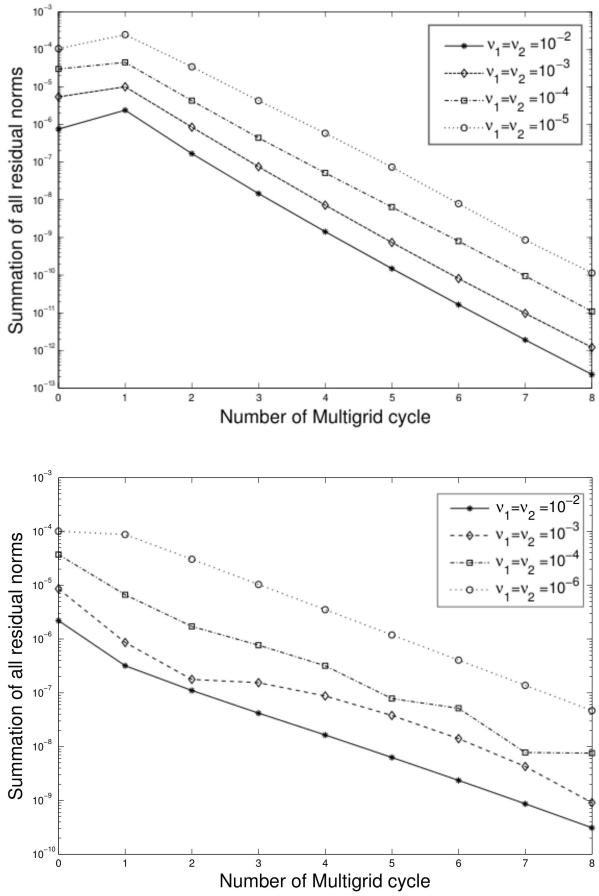


Figure 1: Convergence history of multigrid scheme for different weights. Coarse mesh (upper) and fine mesh (lower).

mesh size, we see that the multigrid scheme does not converge for very small weights such that $\nu \approx h^4$ on the finest triangulation. This can be explained by (4.8), where the factor $(\nu + M_{i,i}^2/K_{i,i}^2)^{-1}$ appears. As ν becomes smaller than $M_{i,i}^2/K_{i,i}^2$, which is actually equal to $4h^4$ for linear triangular elements, the weight looses its influence and the scheme fails to converge.

Further, we investigate the effectiveness of the multigrid framework over the smoothing iterations. We compare the number of iterations against the comparable workload needed to reach a particular accuracy, i.e. the total residual norm of the state and adjoint equations.

From Fig. 2, we can see the multigrid speed-up in different cases. For different mesh sizes, we observe a weak dependence of the convergence rate on the mesh size and on the values of the weights ν_1 and ν_2. These results correspond to control-constrained problems where the controls are partly active. Similar results are observed in control-

https://doi.org/10.4208/nmtma.2015.w11si Published online by Cambridge University Press

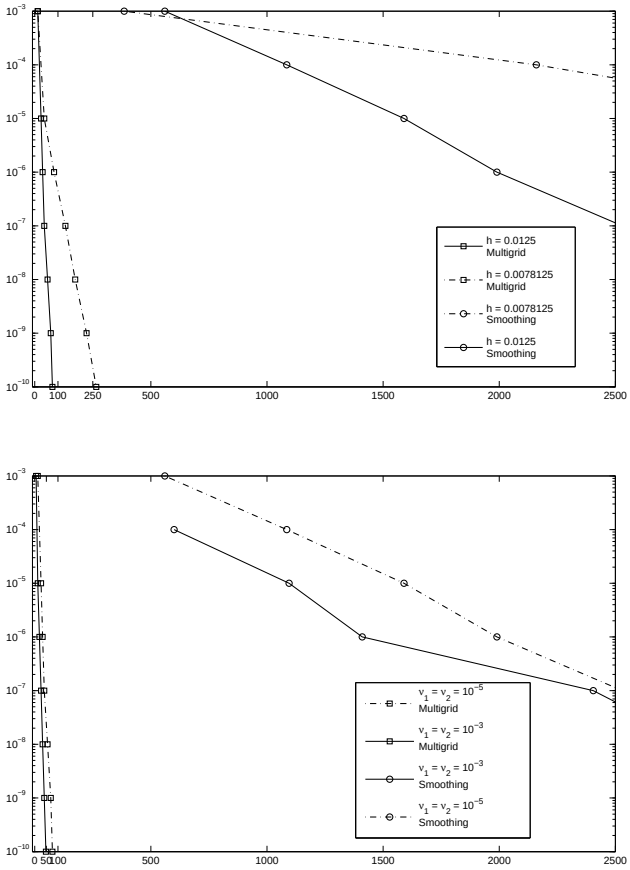


Figure 2: Multigrid acceleration for different mesh sizes (upper) and weights (lower).

unconstrained cases.

Next, we present in Table 4 the comparison of the values of $\eta(TG_k^{k-1})$, obtained from the two-grid local Fourier analysis and from numerical experiments with the same parameters. Concerning the experimental values, the observed value of the convergence factor is defined as the ratio between the L^2 norms of the residuals resulting from two successive multigrid cycles on the finest mesh.

It is clear from the results in Table 4 that the convergence factor improves with additional pre- and post smoothing iterations. Further, we observe the effect of different weights (ν_1, ν_2) as well as different mesh sizes. The convergence factors from the local Fourier analysis provide upper bounds for the convergence factors. As it is observed from the Fourier analysis, three pre- and post-smoothing should be employed for good convergence results, from the experiment it is evident that, two pre- and post-smoothing operations are sufficient.

We finish this section with an example illustrating the application of finite element

https://doi.org/10.4208/nmtma.2015.w11si Published online by Cambridge University Press

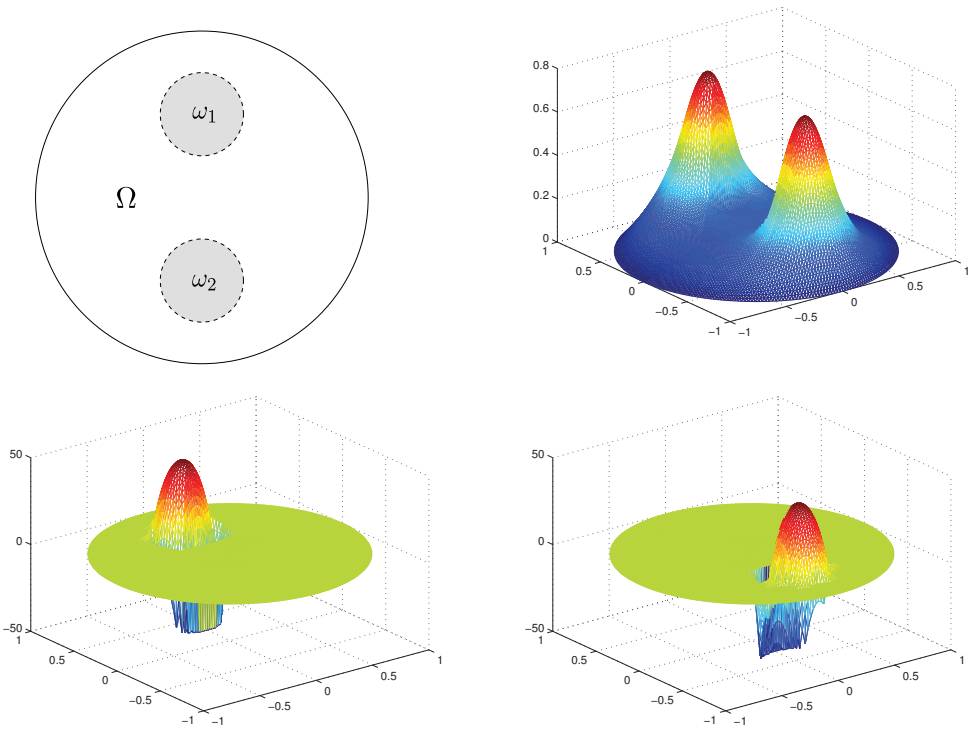


Figure 3: The domain (upper left), results of the computed problem- the state (upper right), the two controls (lower left and right).

Table 4: Convergence factors, from local Fourier analysis and from experiments.

h	(υ_1,υ_2)	$\nu_1=\nu_2=0.01$		$\nu_1=\nu_2=0.001$	
		ρ_{LFA}	$\rho_{Exp.}$	ρ_{LFA}	$\rho_{Exp.}$
1/16	(1,1)	0.315	0.187	0.428	0.187
	(1,2)	0.226	0.127	0.344	0.126
	(2,2)	0.175	0.091	0.296	0.096
	(3,3)	0.119	0.061	0.235	0.067
1/32	(1,1)	0.282	0.203	0.305	0.205
	(1,2)	0.192	0.142	0.217	0.141
	(2,2)	0.141	0.095	0.166	0.099
	(3,3)	0.093	0.078	0.112	0.096

formulation to model domains with complex geometry. In this example our computational domain is a circle with its center at $(0,0)$ and with a radius of 1. Our sub-domains are also circles with radius 0.25 and their centers located in $(0,\pm 0.5)$. The target func-

https://doi.org/10.4208/nmtma.2015.w11si Published online by Cambridge University Press

Table 5: Accuracy

	L^2 residual Norm		
h	State equation	Adjoint equation 1	Adjoint equation 2
0.0625	$2.371 \cdot 10^{-4}$	$2.214 \cdot 10^{-6}$	$2.213 \cdot 10^{-6}$
0.03125	$6.076 \cdot 10^{-5}$	$5.110 \cdot 10^{-7}$	$5.107 \cdot 10^{-7}$
0.015625	$2.583 \cdot 10^{-7}$	$1.273 \cdot 10^{-9}$	$1.255 \cdot 10^{-9}$

Table 6: Tracking property

$\| y - z_1 \|^2_{L^2}$	$\| y - z_2 \|^2_{L^2}$	ν_1	ν_2
$161.9 \cdot 10^{-3}$	$161.9 \cdot 10^{-3}$	10^{-2}	10^{-2}
$158.6 \cdot 10^{-3}$	$158.6 \cdot 10^{-3}$	10^{-3}	10^{-3}
$152.2 \cdot 10^{-3}$	$152.2 \cdot 10^{-3}$	10^{-4}	10^{-4}
$236.2 \cdot 10^{-3}$	$95.5 \cdot 10^{-3}$	10^{-2}	10^{-4}
$183.1 \cdot 10^{-3}$	$131.4 \cdot 10^{-3}$	10^{-3}	10^{-4}

tions are defined as follows

$$z_j := \begin{cases} 1 & \text{if } (x_1, x_2) \in \omega_j \\ 0 & \text{otherwise} \end{cases} \quad \text{for } j = 1, 2.$$

Table 5 shows the residual norm of the state and adjoint equations after 3 multigrid cycle for different mesh size and for the weights $(10^{-1}, 10^{-4})$. In Table 6, the optimization properties are illustrated. Alike the previous examples, the state is closer to the target functions for smaller weights of the costs of the controls.

These results show the ability of the proposed multigrid scheme to model complex domains.

7. Conclusion

An efficient and robust finite-element full multigrid scheme for elliptic Nash-equilibrium multiobjective optimal control problems with control constraints was investigated. Corresponding to the case of two objectives and two controls, the optimality system characterizing the solution of the multiobjective control problem was formulated and discretized by finite elements. It was proved that the FEM optimal controls are $3/2$-order accurate. To compute these optimal controls, a nonlinear full multigrid scheme with collective smoothing was developed. A local Fourier analysis was performed for the smoothing algorithm as well as for a two level multigrid setting. Results of numerical experiments were presented to demonstrate the effectiveness of the proposed framework and to validate the computational performance of the proposed solution strategy. The effectiveness of the FEM multigrid scheme to model complex geometries was demonstrated by numerical experiments.

https://doi.org/10.4208/nmtma.2015.w11si Published online by Cambridge University Press

Acknowledgments This work was supported in part by BMBF Verbundprojekt 05M2013 'ROENOBIO: Robust energy optimization of fermentation processes for the production of biogas and wine', and in part by the European Union under Grant Agreement Nr. 304617 'Multi-ITN STRIKE- Novel Methods in Computational Finance'.

References

[1] A. Borzì and C. Kanzow, *Formulation and numerical solution of nash equilibrium multiobjective elliptic control problems*, SIAM J. Control Optim., 51(2013), 718-744.
[2] A. Borzì and V. Schulz, *Computational optimization of systems governed by partial differential equations*, SIAM book series on Computational Science and Engineering 08, SIAM, Philadelphia, PA, 2012.
[3] A. Borzì and K. Kunisch, *A multigrid scheme for elliptic constrained optimal control problems*, Comput. Optim. Appl., 31 (2005), pp. 309–333.
[4] A. Brandt, *Multigrid Techniques: 1984 Guide with Applications to Fluid Dynamics*, GMD Studies 85, GMD-FTT, 1985.
[5] U. Trottenberg and A. Schuller, *Multigrid*, Academic Press, Inc., Orlando, FL, 2001.
[6] M. S. Gockenbach, *Understanding and implementing the finite element method*, SIAM 2006.
[7] A. Chinchuluun, P.M. Pardalos, A. Migdalas, and L. Pitsoulis (Eds.), *Pareto Optimality, Game Theory, and Equilibria*, Springer, 2008.
[8] S. Dempe, *Foundations of Bilevel Programming*, Kluwer Academic Press, Dordrecht, 2002.
[9] J.-A. Désidéri, *Cooperation and competition in multidisciplinary optimization. Application to the aero-structural aircraft wing shape optimization.* Comput. Optim. Appl., 52 (2012), pp. 29–68.
[10] M. Ehrgott, *Multicriteria Optimization*, Springer, 2nd edition 2005.
[11] N. Gauger, C. Ilic, S. Schmidt and V. Schulz, *Non-parametric aerodynamic shape optimization*, in G. Leugering, S. Engell, A. Griewank, M. Hinze, R. Rannacher, V. Schulz, M. Ulbrich, and S. Ulbrich (eds.), Constrained Optimization and Optimal Control for Partial Differential Equations, International Series of Numerical Mathematics, vol, 160, pp. 289–300, Birkhäuser 2012.
[12] J.L. Lions, *Controle de Pareto de systemes distribues: Le cas d'evolution.* Comptes Rendus de l'Academie des Sciences, Serie I, 302 (1986), pp. 413–417.
[13] G.P. Liu, J.B. Yang, and J.F. Whidborne, *Multiobjective Optimisation and Control*, Research Studies Press LTD, 2001.
[14] A.M. Ramos, R. Glowinski, and J. Periaux, *Nash equilibria for the multiobjective control of linear partial differential equations*, J. Optim. Theory Appl., 112 (2002), pp. 457–498.
[15] A.M. Ramos, R. Glowinski, and J. Periaux, *Pointwise control of the Burgers equation and related Nash equilibrium problems: Computational approach.*, J. Optim. Theory Appl., 112 (2002), pp. 499–516.
[16] A. Rösch, *Error estimates for linear-quadratic control problems with control constraints*, Optimization Methods and Software 21 (2006), 121–134.
[17] W. Stadler, *Fundamentals of multicriteria optimization*, In Multicriteria optimization in engineering and in the sciences, volume 37 of Math. Concepts Methods Sci. Engrg., pages 1–25. Plenum, New York, 1988.
[18] M. Hintermüller and T. Surowiec, *A PDE-constrained generalized Nash equilibrium problem with pointwise control and state constraints.*, Pacific J. on Optimization 9(2), 251-273, 2013

https://doi.org/10.4208/nmtma.2015.w11si Published online by Cambridge University Press